TH-PM-G1 SPATIAL SEPARATION OF CONFORMATIONAL STATES IN UNIMOLECULAR PROTEIN TRANSITION PROCESSES. R. M. Mitchell*and S. A. Hawley‡ Jefferson Physical Laboratories, Harvard University, Cambridge, Massachusetts 02138 Intr. by F. Dunn, University of Illinois, Urbana, Illinois.

The possibility of achieving physical separation of distinct conformations of a single protein in an external field--for example, by electrophoresis--has been examined both experimentally and theoretically. Studies of the electrophoretic separation of the native and reversibly denatured forms of chymotrypsinogen at elevated hydrostatic pressure suggest that this transition process involves only two principal conformational states. Transitory intermediate conformations are not precluded, however, and an upper limit for their lifetime can be determined from experimental information.

TH-PM-G2 EFFECT OF INTERNAL FLUCTUATIONS IN ELECTRON DENSITY ON LOW ANGLE X-RAY SCATTERING FROM DILUTE PROTEIN SOLUTIONS. W. L. Mattice and D. K. Carpenter, Departments of Biochemistry and Chemistry, Louisiana State University, Baton Rouge, Louisiana 70803

The influence on the low angle X-ray scattering due to fluctuations in electron density within rigid macromolecules was studied by numerical calculations for fifteen proteins. The intramolecular scattering function can be resolved into contributions which arise from (1) shape of the protein alone (2) fluctuations in the electron density within the protein (3) a cross term. The relative importance of these contributions depends on the particular structure of the protein and the electron density of the solvent. In water, the radii of gyration calculated are usually larger (up to 6%) than those which correspond to the particle shape. The effects observed arise from the tendency of the amino acid residues of low electron density to be found close to the center of the protein. Most of the calculations assumed that the scattering centers of the protein were located at the alpha carbon atoms of the amino acid residues.

TH-PM-G3 A THEORETICAL ESTIMATE OF THE ENERGY BARRIERS BETWEEN STABLE CONFORMATIONS OF THE PROLINE DIMER AND METHYLPROLINE DIMERS. B.J. Price* and C.M. Venkatachalam, Harrison M. Randall Laboratory of Physics, Biophysics Research Division and Macromolecular Research Center, University of Michigan, Ann Arbor, Michigan 48104.

The puckering of the pyrrolidine ring and its effects on the Pro-Pro internal dipeptide have been studied using semi-empirical energy calculations. The energy of the dimer has been obtained as a function of the backbone torsion angles; ψ,ω. There are three stable conformations available to the dimer; designated cis (ψ=160°, ω=0°), trans (ψ=160°, ω=180°) and cis' (ψ=-40°, ω=180°). Evidence from viscosity studies suggests the existence of the cis' conformation in poly-L-proline while NMR studies indicate only two resonances, attributed to the cis and trans conformations. It is of interest here to determine the barriers separating the three stable conformations. Model building with planar residues shows that cis' is separated from trans (and cis also) by a large barrier of at least 100 kcal/mole, while the trans-cis barrier height is only 20 kcal/mole. Calculations presented here show that if several differently puckered conformations are available to the prolyl rings, the trans-cis' barrier height is comparable to the trans-cis barrier height. This supports the claim of Mattice et. al.[1] that the cis' conformation is present in poly-L-proline. On this basis, one would expect three separate resonances in the NMR spectrum. Similar calculations have been done for the 5-methyl proline dimer with the methyl group in either the cis or trans position, where it is found that the cis' structure is not possible. Further details on these calculations will be presented.

1. W.L. Mattice, K. Nishikawa, and Ooi,T., Macromolecules 6, 443 (1973).

TH-PM-G4 THE OBSERVATION OF CIS-RESIDUES IN POLY-L-PROLINE BY PROTON FOURIER TRANSFORM NMR. C. C. Wu*, R. A. Komoroski, and L. Mandelkern, Department of Chemistry and Institute of Molecular Biophysics, Florida State University, Tallahassee, Florida 32306.

By using high sensitivity Fourier transform proton NMR at 270 MHz, we have observed a resonance at 4.3 ppm in three widely different molecular weight samples of poly-L-proline in D_2O. The intensity of this resonance is about 2-3% of the Cα-trans proton resonance for molecular weights of 1,800, 16,300, and 97,000. On the basis of previous studies of the cis-trans isomerization of poly-L-proline in D_2O, Torchia and Bovey have assigned the resonance at 4.3-4.4 ppm to the cis configuration of the Cα protons. On the basis of this assignment, we can conclude that the resonance at 4.3 ppm that is found here in the spectrum for the chain predominantly in the trans configuration represents randomly distributed cis peptide bonds. The presence of a small proportion of cis peptide bonds will, however, exert a major influence upon the unperturbed chain dimensions and could be a major contributor to the relatively low characteristic ratio that has been determined for this polypeptide. The possibility that the observed resonance corresponds to the Cα-trans protons occupying another rotational state is also consistent with the observed characteristic ratio. The precautionary steps that have been taken to insure the experimental reality of this resonance will be discussed.

TH-PM-G5 THE NORMAL VIBRATION FREQUENCIES OF CRYSTALLINE POLYGLYCINE I: EVIDENCE FOR A RIPPLED SHEET STRUCTURE. W. H. Moore* and S. Krimm, Department of Physics, University of Michigan, Ann Arbor, Mich. 48104.

The structure of crystalline polyglycine I (PG I) has heretofore been assumed to be an antiparallel chain pleated sheet. Recent electron diffraction studies[1] suggest that the structure is more likely to be an antiparallel chain rippled sheet[2]. We have done optimized normal vibration analyses for these two structures, and we conclude that the rippled sheet structure is indeed more compatible with the vibrational spectroscopic data. This is based on the evidence that this structure permits: 1) a better understanding of the high N-H stretching frequency, 2) the prediction of the low amide II frequency (which can be accounted for, together with the higher frequencies of other pleated sheet beta polypeptides, by the same force field), and 3) more reasonable assignments of the low frequency infrared and Raman bands. These studies emphasize the importance of an analysis of the low frequency region of the vibrational spectrum in deriving conformational and structural information.

1. B. Lotz, J. Mol. Biol. 87, 169 (1974).
2. L. Pauling and R. B. Corey, Proc. Nat. Acad. Sci. 39, 253 (1953).

This research was supported by National Science Foundation grants GB-15682 and GP-38093.

TH-PM-G6 DENSITY OF VIBRATIONAL STATES AND LOW TEMPERATURE SPECIFIC HEAT OF POLYGLYCINE.*
Bruno Faconi*, National Bureau of Standards, Polymer Crystal Physics Section, Washington, D.C. 20234, Leonard Finegold, Department of Physics & A.S., Drexel University, Philadelphia, Penna. 19104 and University of Colorado and E.A. Billard*, Univ. of Co. (Intr. by Thomas F. Anderson).

The density of vibrational states has been calculated for the parallel chain hexagonal lattice of 3_1 helical polyglycine. A valence force field has been used for the intrachain interactions and only hydrogen bonding interactions have been included in the interchain force field. Differences in the low frequency density of states of the two crystalline modifications of polyglycine can be attributed to variations in hydrogen bonding. The low temperature specific heat of 3_1 helical polyglycine calculated from the density of states exhibits an anomaly near 8 K in excellent agreement with the experimental results.

*Supported by National Science Foundation grant GB 25963.

TH-PM-G7 NMR INVESTIGATION OF THE WATER-PROTEIN INTERACTION IN PROTEIN CRYSTALS. Edward S. P. Hsi and R. G. Bryant*, Department of Chemistry, University of Minnesota, Minneapolis, Minnesota 55455. 373-5575

Nuclear magnetic resonance investigations of water in protein crystals permits direct deductions concerning the dynamics and the range of the interaction between water and protein. The transient response of the nmr signal may be resolved into a minimum of three components which correspond to distinct populations of protons associated with water and exchangable protein protons. Two of these relaxation components are associated with the protein surface, one with the aqueous internal solution of the crystal. Only one of the protein surface phases of water exchanges with the liquid fraction; however, both of the protein surface phases have a great deal of motional freedom even though there are severe constraints in the lifetime of the water molecules in each phase. The small spaces between protein molecules in the protein crystal permits a direct accessment of the range over which the perturbation of water structure extends and the data clearly show that in terms of the water molecule dynamics it is on the order of one or two monolayers of water only. A quantitative description of the water interactions will be presented. This work was supported by the National Institutes of Health GM18719, GM21335.

TH-PM-G8 ^{1}H NMR IN AQUEOUS SOLUTIONS OF POLY L LYSINE HBr. D. R. Woodhouse[a] and W. Derbyshire[b], Department of Physics, University of Nottingham, Nottingham, NG72RD, United Kingdom. (introduced by Prof. D. O. Shah)

Aqueous solutions of polypeptides are convenient model systems for investigations of protein hydration. In the work reported here the ^{1}H NMR spin-lattice and spin-spin relaxations of aqueous solutions of poly L lysine HBr have been recorded as functions of chain length, concentration and temperature. Below the freezing point the amount of unfrozen water was observed to be proportional to poly lysine concentration, and to exhibit an exponential inverse temperature dependence. Somewhat unexpectedly the gradients showed a chain length dependence for which no explanation is offered. Above 0°C graphs of T_2 values against temperature exhibited maxima and minima even for those samples where the water content was sufficiently low that freezing did not occur below 0°C. The occurrence of such maxima and minima in the T_2-temperature plots was attributed to exchange between water and side chain N^+H_3 protons and confirmed by high resolution NMR.

[a]Now at Unilever Research Laboratories, Greyhope Road, Aberdeen, Scotland

[b]Now on leave at Department of Physics and Astronomy, University of Florida, Gainesville, FL 32611, U. S. A.

TH-PM-G9 STUDIES ON THE MECHANISM OF FLUORESCENCE QUENCHING OF β-TRYPSIN AT ALKALINE pH VALUES. C. A. Ghiron and N. Ramachandran*, Dept. of Biochemistry, University of Missouri, Columbia, Missouri 65201.

The tryptophanyl fluorescence of proteins invariably decreases with increasing pH values. Since phenolate absorbs at longer wavelengths than indole sidechains, it has been proposed that alkaline quenching of proteins is largely accounted for by resonance energy transfer from indole to phenolate. Direct proof of this mechanism is difficult to obtain because the ionized tyrosinyl residues fluoresce in approximately the same spectral region as tryptophanyl residues but with a yield that is an order of magnitude less. Evidence for this mechanism must come indirectly from experiments that minimize the involvement of hydroxyl ions and the ε-amine groups of lysine as quenchers. The present work is an attempt to analyze the alkaline quenching of β-trypsin fluorescence. The viscosity of the solvent was increased by the inclusion of 40% sucrose. The fluorescence lifetime and yield of β-trypsin were determined in the pH range 7 to 11.5. The competitive inhibitor cyclohexylcarboxamidine was used to stabilize the native conformation of this enzyme and to prevent autolysis in this pH range. Energy transfer from indole to phenolate is shown to be the predominant alkaline quenching mechanism in β-trypsin because increasing the number of phenolate sidechains by increasing the pH leads to a per cent decrease in the tryptophanyl fluorescence lifetime equal to that of the fluorescence yield. Further, the solvent viscosity does not influence the dependence of the fluorescence yield on the fractional ionization of tyrosinyl residues. (These results are inconsistent with either a collisional or a static quenching mechanism (i.e. hydroxyl ion and/or ε-amino groups quenching)).

TH-PM-G10 CONFORMATIONAL FLEXIBILITY OF STAPHYLOCOCCAL ENTEROTOXIN A. J.R. Warren and J.F. Metzger*, Department of Pathology and Oncology, University of Kansas Medical Center, Kansas City, Kansas, and U.S. Army Medical Research Institute of Infectious Diseases, Frederick, Maryland.

The large kinetic stability of staphylococcal enterotoxin B (SEB) toward isothermal unfolding by the protein denaturant guanidine hydrochloride (Gdn·HCl) suggests a rigid native toxin conformation (Warren et al., Biochemistry, 13, 1678, 1974). To define possible relationships between configurational stability and *in vivo* expression of enterotoxicity, we have investigated the behavior of another staphylococcal enterotoxin variant (SEA) in aqueous solutions of Gdn·HCl. This variant was chosen since the enterotoxicity of SEA for rhesus monkeys significantly exceeds the toxicity of SEB (Schantz et al., Biochemistry, 11, 360, 1972). Unfolding of SEA was followed at 24° by change in the reduced viscosity and near-ultraviolet difference spectrum of the exoprotein. An increase in reduced viscosity to values typical of extensively unfolded protein and a denaturation "blue-shift" of the difference spectrum with minima at 287 nm and 279-281 nm were obtained by SEA between 1 M and 2 M Gdn·HCl. SEB unfolded only at concentrations of Gdn·HCl greater than 2 M. Kinetic analysis of the rate of decrease in difference molar absorbancy at 287 nm was compatible with apparent first-order kinetics for SEA unfolding over a wide range of Gdn·HCl concentration. Calculated values for the rate constants of SEA unfolding above 2 M Gdn·HCl were several hundred-fold larger than those values reported previously for SEB. It appears, therefore, that: (1) the SEA molecule does not possess the unusual conformational stability toward Gdn·HCl denaturation demonstrated by the SEB molecule; (2) configurational flexibility and biologic toxicity increase in parallel for these staphyloccal enterotoxins.

TH-PM-G11 TEMPERATURE JUMP NMR STUDY OF INTERMEDIATES IN REFOLDING OF RIBONUCLEASE. A. Blum*, S. H. Smallcombe*, R. L. Baldwin, Department of Biochemistry, Stanford Medical Center, Varian Associates, Palo Alto, California.

A temperature-jump proton NMR study provides direct physical evidence for kinetic intermediates in the refolding of bovine pancreatic ribonuclease A. The unfolded protein (45°C, pH 1.8) is cooled rapidly to 10°C. Data acquisition is begun within 20 seconds. The half life for refolding to the native conformation at 10°C is several minutes, providing sufficient time to monitor the changes in the C-2 histidine region by Fourier Transform NMR. Two interesting phenomena are observed during refolding. (1) The native peaks assigned[1] to His 119 and His 48 reappear at a more rapid rate than the composite peak assigned to His 12 and 105. (2) Two non-native peaks appear whose chemical shifts are close to that of the single peak found for all four histidines in the denatured protein. These peaks disappear upon complete refolding. These phenomena, in particular the appearance of a peak found neither in the native nor in the denatured spectrum of ribonuclease A, provide direct evidence for a kinetic intermediate. A model is proposed whereby rapid formation of this intermediate is followed by slow conversion to the native conformation during several minutes. We thank Dr. C. R. Matthews for advice and discussion. This work was supported by research grants from N. I. H. and N. S. F.

[1] Meadows, D. H., et al. (1968). Proc. Nat. Acad. Sci. 60, 766-772.

TH-PM-G12 TRANSPORT AND INTERACTION OF PROTEINS IN POLYANIONIC GELS: Santibrata Ghosh, David B. Moss‡ and John S. Schweppe‡ Northwestern University Medical and Dental Schools, Chicago, Illinois 60611.

The behavior of several proteins: serum albumin (SA) and low and very low density lipoproteins (LP) during electrophoresis in polyanionic gels was examined as a model for their transport and interaction in the tissue matrix. Gels were prepared from: (a) agarose, (b) agar and (c) agarose plus a mucopolysaccharide (MPS) chondroitin sulfate, hyaluronic acid or heparin. Electroendosmotic mobilities (EO) determined in these gels showed the charge density of the molecules in the gel phase to be more negative in MPS-agarose and in agar than in agarose. The values of the electrophoretic mobility of the proteins determined in gels of different concentrations were analyzed in terms of the Ferguson equation: $M_0 = M_T \exp(-K_r T)$, where M_0 and M_T are mobilities at gel concentrations zero and T respectively, and K_r the retardation coefficient. We have recently reported that K_r is independent of EO whereas to get the true electrophoretic mobility M_{cor}, M_0 has to be corrected for EO. The present data show that despite differences in M_0, M_{cor} for SA was constant, indicating no complex formation with polyanionic material. For LPs both M_{cor} and K_r were elevated in agar and in most MPS containing gels due to interaction between LP and MPS. Studies at varying concentration of NaCl showed higher mobilities in MPS-gels than in agarose; these results indicate the formation of soluble complex between LP and MPS even at physiological ionic strength and even in the absence of Ca^{++}.

TH-PM-G13 STUDIES OF THE DYNAMIC SURFACE TENSION OF PLASMA LIPOPROTEINS. Benjamin J. An* and J. L. Oncley, Biophysics Research Division, Institute of Science and Technology, University of Michigan, Ann Arbor, MI 48105.

Experimental evidence regarding the rate of exchange of lipids between plasma lipoproteins and membranes indicates that the interaction probably involves some deformation of the lipoprotein molecules and reorientation of specific groups in the macromolecules at interfaces. In an attempt to study this problem we have used the pendant drop method to obtain dynamic surface tensions of aqueous solutions (air interface) of human α-lipoprotein(HDL) and β-lipoprotein(LDL). These measurements are compared with similar studies which we have made on bovine serum albumin(BSA), bovine insulin(BIN) and poly-N ^{5}-(3-hydroxylpropyl)-L-glutamine(PHPG), and with literature values for egg-white ovalbumin(EWO) and egg-white lysozyme(EWL).

Surface tensions are extrapolated to infinite time, and then plots of surface pressure (equal to the difference of surface tension between solvent and solution) are prepared as a function of $\ell n[c]$ (where c is the concentration of macromolecule in g/ml). Linear variations are observed in a high concentration range ($c>10^{-4}$), with surface pressure values for the various macromolecules in the order EWO>LDL>HDL>BSA>PHPG>HWL (BIN not completed). The curves fall precipitously in a low concentration range ($c<[2.5\pm1.5]\times10^{-5}$) to surface pressures near zero.

Interpretation of these results are in a rather primitive state, but we have tested various surface equations of state combined with the Gibbs adsorption equation, and thus investigated possible ranges of parameters (molecular surface area, coordination number, etc.) used in these equations. The kinetics of the dynamic surface tension was investigated and compared with that predicted by the diffusion limited case, using the spherical diffusion equation under proper boundary conditions.

TH-PM-H1 ULTRA VIOLET CARCINOGENESIS. P. Rosen , Oak Ridge National Laboratory and University of Massachusetts, Amherst, Massachusetts 01002.

A theoretical model for the experiments of R. Hart and R. Setlow[1,2] is proposed. Homogenates of tissue from the fish Poecelia formosa are subjected to UV and injected into live fish from the same clone. The number of transformed cells can be measured in this experiment. Assuming excision repair is negligible and immunological factors are blocked, the probability of transformation can be calculated by assuming that DNA damage occurs in the form of pyrimidine dimers in a critical operator controlling the synthesis of divisional proteins. Errors occur either in replication or in post replication repair so that derepression occurs as well in daughter cells. We obtain the equation $N_{TTC} = rN_oKLDf$ for the number of initial tumor cells from N_o original cells. Here $K = 10^{-6}$ dimers/BP erg/mm^2, L = 20 B.P., D = Dose, f is the mutation frequency per unexcised dimer and r is the surviving fraction. Experiment on thyroid cells yields 1 in 10^5 cells transformed at 50 erg/mm^2. Using a value for $f = 1/2 \times 10^3$ [4] for E. Coli and a ratio of 50:1 for mutation frequency for fish compared to E. Coli[3] we find 2.5 cells in 10^5 transformed ($r = 1$).

Supported by NIH Fellowship 1F03CA52956-01 from National Cancer Institute

1. R. Setlow and R. Hart, 1975, Proceedings 5th International Congress of Radiation Research, Seattle.
2. R. Hart and R. Setlow, 1975, Symposium Squaw Valley, Molecular Mechanisms for Repair of DNA.
3. S. Abrahamson et al., 1973, Nature 245, 460.
4. E. Witkin, 1969, Ann. Rev. Genet. 3, 525.

TH-PM-H2 ENDONUCLEASE SENSITIVE SITES IN UV-IRRADIATED DNA. R. B. Setlow, Biology Department, Brookhaven National Lab., Upton, N. Y. 11973, and W. L. Carrier, Biology Division, and Juarine Stewart*, University of Tennessee-Oak Ridge Graduate School of Biomedical Sciences, Oak Ridge National Lab., Oak Ridge, Tenn. 37831.

An endonuclease from M. luteus makes single strand breaks in DNA containing pyrimidine dimers, and the enzyme has been used in several studies to estimate the numbers of endonuclease sensitive sites in DNA that has undergone repair in vivo. However, there have been no precise determinations indicating that the enzyme attacks every dimer. We used two different DNAs and several wavelengths to measure the ratio of sites to dimers. Measurements of the amount of unnicked polynucleotides of the circular duplex DNA of phage PM2 labeled with dThd indicated that the number of nuclease-sensitive sites corresponded to 1.0 ± 0.1 dimer. The total number of dimers was estimated from the number of thymine-containing ones. These experiments would not have detected any effect due to clusters of dimers. We also used purified E. coli DNA labeled with both dThd and dCyd and measured directly total dimers by chromatography and enzyme sites from number-average molecular weights obtained by sedimentation in alkaline gradients that had been calibrated with 5 phage DNAs. Fractions at the top corresponding to $M < 30,000$ were ignored. Hence dimer clustering might lead to an underestimation of the number of breaks. For seven determinations we found 0.99 ± 0.08 sites per dimer and we conclude that every dimer is recognized by the enzyme and that dimer clustering is not an important consideration in E. coli DNA. (This work was sponsored by the U. S. Atomic Energy Commission at Oak Ridge National Laboratory under contract with Union Carbide Corporation.)

TH-PM-H3 INHIBITION BY ULTRAVIOLET LIGHT OF SEMICONSERVATIVE DNA SYNTHESIS IN HELA CELLS. Howard J. Edenberg, Department of Biology, Massachusetts Institute of Technology, Cambridge, Massachusetts 02139.

The inhibition by ultraviolet light (UV) of semiconservative DNA synthesis in HeLa cells has been examined by two different methods. Isopycnic gradient analysis was used to separate incorporation due to semiconservative synthesis from that due to repair synthesis; and DNA-fiber autoradiography was used to examine the spatial arrangement of the post-irradiation synthesis. The isopycnic analysis showed the inhibition to vary with time. After low doses of UV (below 10 J/m^2) the initially depressed rate of DNA synthesis later rose. After higher doses, synthesis continued at a constant, low rate for at least 6 hours. Examination of the DNA-fiber autoradiograms revealed that the average length of DNA synthesized in the first 1.5 hours after irradiation decreased with increasing UV dose, as expected. For a given dose, the lengths increased more rapidly in the first few 10 minute intervals after irradiation, and then the increases slowed.

TH-PM-H4 SINGLE-STRAND BREAKS IN DNA FROM UV-IRRADIATED WILD TYPE AND UV SENSITIVE STRAINS OF SACCHAROMYCES CEREVISIAE. R.J. Reynolds*. (Intr. by Robert S. Stafford), The University of Tenn.-Oak Ridge Grad. Sch. of Biomed. Sci., Biology Division, Oak Ridge National Laboratory, Oak Ridge, Tenn., 37830.

The inability of the ultraviolet sensitive rad 1 and rad 2 mutants of Saccharomyces cerevisiae to remove dimers from their DNA after UV irradiation (Unrau et al., Mol. Gen. Genet. 113:359, 1971; Resnick and Setlow, J. Bacteriol. 109:979, 1972) suggests these mutants have defects in an excision repair pathway. The rad 3 and rad 4 genes have also been implicated in the same pathway (Game and Cox, Mut. Res. 16:353, 1972). A modification of the McGrath and Williams alkaline sucrose gradient technique for detecting single-strand breaks in DNA has been employed in an attempt to better understand the role of these genes. UV-irradiated cells were held in .067 M KPO_4, pH 7.0, for various periods, lysed on top of alkaline sucrose gradients, and the DNA sedimented. In the haploid wild type strain S288C, strand breaks appear rapidly during the post-irradiation incubation, reach a maximum number, and subsequently decrease again. Both the maximum number of breaks observed and the length of incubation required before they are no longer detected increase with fluence. The appearance and disappearance of strand breaks was most notably affected, relative to the wild type, in rad 3 and rad 4 mutants. The data indicate that the rad 3 mutation affects an early step in the excision repair pathway.

(Research sponsored by the U.S. Atomic Energy Commission under contract with the Union Carbide Corporation).

TH-PM-H5 UV MUTAGENESIS IN RADIATION SENSITIVE STRAINS OF YEAST. C.W. Lawrence and R. Christensen*, Department of Radiation Biology and Biophysics, University of Rochester Medical Center, Rochester, New York 14642.

The involvement of different repair pathways in UV mutagenesis, and also their specific action, has been studied in the yeast Saccharomyces cerevisiae by determining the reversion frequency of a defined mutation in twenty-seven diploid strains, each homozygous for a different non-allelic radiation sensitive mutation, by constructing strains carrying two different radiation sensitive mutations (double mutant analysis) and by examining reversion of two different defined mutations. The results suggest that UV mutagenesis in yeast depends on the action of a single "error-prone" repair pathway, which can be blocked by mutation at a minimum of six loci, namely rad6, rad9, rad18, rev1, rev3, and probably rev2. The function of the RAD6 gene would appear to be required for UV mutagenesis of all kinds and at all sites in the genome, and the same is probably true of the REV3 locus. The rad6 rev3 double mutant was completely UV immutable to a resolution better than 1 in 10^9. The function of the other genes, however, would appear to be required for only certain mutational events, in that defective alleles at these loci reduced the frequency of induced reversion of only one of the two defined test mutations studied. Strains defective in excision repair all showed reversion frequencies that were higher than normal, suggesting that excision repair is largely error-free. Similarly, the third, minor, UV repair pathway would also appear to be error-free.

This paper is based on work performed under contract with the U.S. Atomic Energy Commission at the University of Rochester Atomic Energy Project and has been assigned Report No. UR-3490-646.

TH-PM-H6 CONTROL OF DOUBLE-STRAND BREAK REPAIR IN DIPLOID YEAST BY THE RAD52 GENE. M.A. Resnick and P. Martin*, University of Rochester, Department of Radiation Biology and Biophysics, Rochester, New York 14642, USA.

The repair of double-strand breaks in the yeast Saccharomyces cerevisiae has been investigated further in terms of the role of the rad52 gene product. In logarithmically growing cells double-strand breaks are induced with single hit kinetics at a frequency of $0.7/10^{10}$ Daltons-krad over the range 25 to 100 krad. The number average molecular weight (M_n) extrapolated to zero dose is 2.4×10^8 Daltons in contrast to an experimentally determined value of 3.1 indicating a sensitive component to double-strand break production. This measured value for unirradiated DNA which is significantly lower than other published reports is based on x in the relationship $(d_i/d_z) = (M_i/M_z)^x$ being experimentally determined as 0.409. The efficiency of repair of double-strand breaks which is approximately 80% at low doses (25 krad) can explain the survival curves obtained with wild-type strains. Cycloheximide does not significantly inhibit this repair; however, at higher doses degradation observed at 6 hours after irradiation is prevented by cycloheximide. Unlike the wild-type strain no repair of double-strand breaks is observed in rad52 strains at 25 krad which appears to explain much of the increase in sensitivity from 15-30 krad for wild-type diploids to 2-2.5 krad for various rad52 strains. The apparent lack of repair in stationary phase cells will also be discussed in terms of these results. In addition results on the importance of the RAD18 gene product in double-strand break repair will be presented. (This paper is based on work performed under contract with the U.S. Atomic Energy Commission at the University of Rochester Atomic Energy Project and has been assigned Report No. UR-3490-645.)

TH-PM-H7 RADIATION INDUCED RELEASE OF NATIVE DNA FROM A NON-FREELY SEDIMENTING COMPONENT OF MAMMALIAN CELLS. R. Chen*, A. Cole, and S. Robinson* (intr. by R. Shalek), Department of Physics, M. D. Anderson Hospital and Tumor Institute of The University of Texas System Cancer Center, Houston, Texas 77025.

When interphase cells, interphase nuclei, or mitotic cells are lysed in sarkosyl to release native DNA to sediment through a 5M NaCl neutral sucrose density gradient only 20 to 30% of the labeled DNA sediments freely and forms a profile which exhibits a peak value at $1.7 \cdot 10^9$ Daltons. The non-freely sedimenting activity is found at the top of the gradient and adhering to the walls of the polyalomer centrifuge tubes. Irradiation of cells with increasing doses prior to lysis causes an increasing amount of DNA to sediment freely such that at 10 Krads a maximal release of 85% of the total activity is found within a similar profile which exhibits a peak at 10^9 Daltons. Incubation of the cells after irradiation and prior to lysis leads to a restoration of the zero dose characteristic, i.e., 70 to 80% of the activity reappears in the non-freely sedimenting fraction. On the other hand, when purified isolated mitotic chromosomes are dissociated in sarkosyl, 80 to 85% of the DNA sediments freely to form a clear profile (peak at $1.7 \cdot 10^9$ Daltons) even when no irradiation exposure is utilized. However, reconstitution of purified chromosomes with isolated supernatant fractions of cell lysates causes the reappearance of the non-freely sedimenting fraction. Thus it appears that a molecular or small particulate component of cellular material associates with chromatin or DNA to form the non-freely sedimenting component. Present studies are designed to isolate and define the specific supernatant component, the sites and mechanism of association, and the mechanism for radiation release of the DNA. Supported in part by AEC (DBER) contract AT-(40-1)-2832

TH-PM-H8 CORRELATION BETWEEN DEFICIENT DNA SYNTHESIS AND CELL KILLING IN X-IRRADIATED HELA S3 CELLS. T.D. Griffiths* and L.J. Tolmach, Departments of Anatomy and Radiology, Washington University School of Medicine, Saint Louis, Missouri, 63110.

It was established previously that irradiation of HeLa S3 cells with 500 rads of 220 kV x-rays 3 hours after mitotic collection (i.e., in early G1 of Generation 0) results in deficient DNA synthesis in the next generation (Generation 1). In the present study two correlations have been found between this deficiency in DNA synthesis and loss of colony-forming ability. (1) The deficiency is dependent on the stage in the generation cycle at which cells are irradiated. The greatest deficiency (55-70% after a dose of 500 rads) is exhibited by cells irradiated at mitosis or at the G1/S transition, and the smallest deficiency (20-35% after 500 rads) is found in cells irradiated in early G1 or early G2. The high sensitivity of cells at the G1/S transition is manifested also by a steeper dose-response than is found in cells irradiated in early G1, and is observable both as depressed incorporation of labeled thymidine per culture (Geiger counts) and as a lowered autoradiographic grain count per cell. This pattern of fluctuations is temporally the same as that for the loss of the ability to survive and form macrocolonies after irradiation. (2) The deficiency in DNA synthesis is enhanced by postirradiation treatment of cells with sublethal concentrations of hydroxyurea. Treatment of early G1 cells with 1 mM hydroxyurea for 17 hours immediately after irradiation with 450 rads increases the deficiency in DNA synthesis from 15 to 50%. Thus, as in the case of cell killing, x-rays introduce potential damage whose expression can be modified by postirradiation conditions. These results suggest that cell killing and deficient DNA synthesis in Generation 1 arise from a common x-ray-induced lesion.

TH-PM-H9 IN VITRO AND IN VIVO EXCISION REPAIR OF GAMMA RAY INDUCED BASE DAMAGE IN HUMAN FIBROBLASTS. M. R. Mattern*, P. V. Hariharan*, and P. A. Cerutti, Department of Biochemistry, University of Florida, Gainesville, Florida 32610.

Diploid human lung fibroblasts WI-38 and SV40-transformed WI-38 were exposed to high doses of gamma radiation and their DNA analysed, following postirradiation incubation, for products of the 5,6-dihydroxy-dihydrothymine-type (t´). Within fifteen minutes of incubation at 37°, 70 to 90 percent of t´ had been removed from acid precipitable DNA in both lines; incubation of WI-38 at 0-4° resulted in only 10-15 percent t´ excision. The amount of DNA degradation induced by ionising radiation varied from one percent in WI-38 to 15 percent in SV40-transformed WI-38 cells. Comparison of DNA degradation with the amount of t´ excision indicates that the process is selective in both lines.

Excision of t´ was also accomplished by isolated nuclei. Nuclei from WI-38 cells were incubated *in vitro* with exogenously supplied gamma-irradiated bacteriophage PM2 DNA or OsO_4-oxidised poly(dAdT) and the acid-precipitable material analysed after 60 minutes of incubation at 37° for the presence of t´-type products. Nuclei from young and intermediate WI-38 cells selectively excised 25-35 percent of t´ within 60 minutes.

This work was supported by the United States Atomic Energy Commission.

TH-PM-H10 STUDY OF RADIOSENSITIVE SITES OF CELLS USING PARTLY PENETRATING α-PARTICLES. R. Datta*, A. Cole, and S. Robinson* (intr. by R. Meyn), Department of Physics, M.D. Anderson Hospital & Tumor Institute of The University of Texas System Cancer Center, Houston, Texas 77025.

Alpha particles from ^{241}Am were used to irradiate CHO cells. The cells were irradiated at different distances from the source (starting from a beam which fully penetrates the cell to that of partially penetrating beams). The depth dose was measured for each distance by an extrapolation chamber. D_{37} doses were determined from the cell survival curves. The data of D_{37} vs the residual α-particle range were compared with data for low energy electron beams. Both show that partially penetrating beams were two to four times more effective for cell killing than fully penetrating beams. An analysis of the present data supports the proposal that the radiosensitive sites are located near the nuclear membrane and not uniformly distributed within the nucleus.

Supported in part by AEC (DBER) Contract AT-(40-1)-2832, and Fellowship 1-F22 CA 01627-01 from the NIH.

TH-PM-H11 THE EFFECT OF INDUCTION OF AN INHIBITION FACTOR ON THE RADIATION SENSITIVITY OF ESCHERICHIA COLI. Ernest C. Pollard and Phillip M. Achey, Biophysics Department, The Pennsylvania State University, University Park, Pa. and Radiation Biology, University of Florida, Gainesville, Fla.

The effect of induction of the inhibitor of post-irradiation DNA degradation on the sensitivity of cells to radiation has been studied. In order to separate the induction process from the radiation damage process, cells were first treated with inducing agents: ultraviolet light, ionizing radiation, or nalidixic acid, allowed to become induced by incubation for 50 minutes and then given rifampin to block further induction. They were then tested for radiation sensitivity. It was found that all strains tested, except recA$^-$, lex$^-$ and recB$^-$ showed very apparent protection. Induction by uv had the most effect and by nalidixic acid the least. The time course of development of protection was observed in one case: it was 50% established in 15 minutes. The absence of an effect in the recA and lex cases is explainable by the fact that these cells cannot be induced. The low protection in the recB case is presumably due to the lack of exonuclease V which is the enzyme inhibited by induction. The cell strains used were W3110, P3478 (polA$^-$), WU 36-10 89 (uvr$^-$), AB1157, AB2463 (recA$^-$), AB2470 (recB$^-$), AB2492 (lex$^-$). Since there is some protection by induction by ionizing radiation against uv it is probable that protection is not only due to inhibition of exonuclease V but that other inducible factors may play a part. The conclusion is reached that the inducible inhibitor of post-irradiation DNA degradation is one factor in the recovery system possessed by E. coli cells.

TH-PM-H12 CHANGES IN LIPID COMPOSITION OF E. COLI FOLLOWING γ- AND UV-IRRADIATION.[1] A.F. Jacobson*[2] and M.B. Yatvin, Radiobiology Research Laboratories, Department of Radiology, University of Wisconsin Medical School, Madison, Wisconsin 53706

The effect of exposure to large doses of ^{137}Cs γ-rays and UV radiation on the lipid composition of E. coli B/r and B_{s-1} was studied. Changes in the relative proportions of the three phospholipids (phosphatidylethanolamine (PE), phosphatidylglycerol (PG), and cardiolipin (CL)) which accounted for more than 97% of the total activity recovered from control cells prelabelled with ^{14}C-acetate were examined in irradiated and reincubated cells. The most sensitive indicator of γ-radiation effects was the CL percentage of the major phospholipids (CL%), which increased markedly following irradiation and reincubation. The magnitude of the increase was a function of both dose and time post-irradiation, with the maximum change being for B/r, from 4% in control cultures to 15% at 180 min following 54krads (the largest dose used). Similar effects appeared in B_{s-1}, but at lower doses than for B/r. Irradiation of B/r with UV at dose levels comparable in cell killing to the γ-doses used produced only one-third as great increases in CL%. In all cases, as CL% increased, the percentage of its probable synthetic precursor PG decreased. At high γ-doses (36krads or greater), the increase in CL% was also accompanied by a significant increase in the amounts of three unidentified lipids, which accounted for more than 8% of the total lipid activity. Post-irradiation pulse-labelling experiments were also performed to study lipid synthesis patterns. Increased conversion of PG and/or decreased CL catabolism are the most likely explanations for the observed increase in CL%. [1]Supported in part by NCI Center Grant # CA-14520. [2]Trainee, NCI Training Grant # 5-T01-CA-05104.

TH-PM-H13 ACUTE AND CHRONIC EFFECTS OF THE ELECTRON AFFINIC RADIOSENSITIZER, METRONIDAZOLE, ON THE HEART RATE AND RECTAL TEMPERATURE OF C3H/HeJ MICE.
M.J. Haynes* and W.R. Inch, Ontario Cancer Treatment and Research Foundation, London Clinic and Department of Biophysics, University of Western Ontario, London, Canada.

Several electron affinic compounds have been shown to be effective sensitizers of radioresistant hypoxic cells in tissue culture. However, most are too toxic for effective use in animals and reduce blood flow and tumor oxygenation. One of the less toxic compounds, metronidazole, was given to 25 gm C3H/HeJ mice (0.6 mg/gm body weight intraperitoneally) twice a day for nine days. Heart rate and rectal temperature were monitored continuously from 30 minutes before to 90 minutes after injection; both variables decreased significantly compared with saline controls. The decrease was greatest on the first day (heart rate dropped 35%, temperature 6.3°C) and became smaller by day seven (heart rate dropped 25%, temperature 3.7°C). Plasma concentrations of metronidazole were determined by spectrophotometry on other mice maintained on the same schedule of drug administration; they decreased from a peak concentration of 3.5 mM on the first day to 2.75 mM by day seven. These data suggested that the animal became tolerant to the chemical with time. This may be important in clinical radiotherapy where the total dose of radiation is given in many fractions over a period of weeks.

Work supported by Ontario Cancer Foundation, London Clinic.

TH-PM-I1 QUANTITATION OF RNA TUMOR VIRUSES BY SPECTROSCOPY OF DENSITY GRADIENT-GELS. L. Liebes*†, E. Retzel*†, M. A. Rich*†, J. J. McCormick*†, I. Salmeen*†† and L. Rimai††, Intr. by S. Horowitz†, † Michigan Cancer Foundation, Detroit, Michigan 48201 and ††Scientific Research Lab., Ford Motor Co., Dearborn, Michigan 48121.

We have developed a system for virus particle quantitation based on the measurement of chromophoric staining of viruses which have been banded at their buoyant density in an equilibrium gradient. The immobilization of mouse leukemia virus (MuLV, Rauscher) and avian myeloblastosis virus (AMV, BAI strain) in 20-53% sucrose density gradients has been obtained routinely by photo-polymerizing an acrylamide riboflavin mixture in the sucrose. With the virus immobilized at its equilibrium density position, the gels are exposed to the protein stain, coomassie blue R250, and subsequently destained. Absorbance profiles reveal the presence of a virus band in the middle of the 20-53% gradient at a density of 1.16 g/cm^3 while extraneous protein material remains in the top 13% of the 4 cm gradient gel. Using plasma from normal and leukemic mice and chickens we have been able to discern virus bands only in the plasma of viremic animals. By using virus stock solutions whose absolute concentrations had been determined by laser beat frequency spectroscopy, we have calibrated the absorbance of the stained viral bands in terms of virus particle counts. The system is linear for viral concentrations up to 2.6 X 10^8 particles/cm^3 for AMV and 9 X 10^7 particles/cm^3 for MuLV. The limits of detection of the system using coomassie blue staining are 2 X 10^7 particles/cm^3. We are investigating the use of fluorescent chromophores which should allow a 10 to 100 fold increase in sensitivity. Supported by NCI, Contract NOI-CP-33226 and an Institutional Grant from the United Foundation.

TH-PM-I2 ELECTRON MICROSCOPIC ASSAY FOR VIRUS PARTICLES FOR EARLY DIAGNOSIS. A. Buzzell, USA Med Res Inst Infectious Dis., Frederick, MD 21701.

Although electron microscopy should be the quickest way to detect and identify virus particles, it has yet to be used in early diagnosis. A principal obstacle for the application to early diagnosis was overcome by Sharp in his method for concentrating virus, free from salts and cell debris, by centrifugation onto agar. However, his technique of stripping virus off by a collodion film, formed on the agar, is cumbersome and often damages the virus structurally. In addition, sensitivity of the assay is limited to concentrations near peak viremia ($\sim 10^6$/ml).

A much easier method for transferring the virus will be described which is far more gentle, since the virus is simply washed down onto the support film. With stain incorporated into the agar, excellent negative staining is possible, for the layer of fluid deposited is thin, drying at once when the agar is removed. Not only is fine structure preserved, with images sharp for every particle, but changes in structure occurring in solution can even be followed, as will be shown.

Since the procedure can be used with millipore filters as well as agar, new methods for concentrating the virus can be tried to increase sensitivity of the assay, probably enough for early diagnosis.

TH-PM-I3 QUANTITATION OF RNA TUMOR VIRUSES BY LASER BEAT FREQUENCY LIGHT SCATTERING SPECTROSCOPY (LBFS): REVERSE TRANSCRIPTASE ACTIVITY PER VIRION FOR AVIAN MYELOBLASTOSIS (AMV-BAI STRAIN) AND MURINE LEUKEMIA (MuLV-RAUSCHER) VIRUSES. I. Salmeen and L. Rimai, Sci. Res. Staff, Ford Motor Co., Dearborn, MI 48121. L. Liebes*, M. A. Rich* and J. J. McCormick*, Michigan Cancer Foundation, Detroit, MI 48201. (Introduction by T. Cole)

The autocorrelation function obtained by LBFS (homodyne detection) consists of two exponentials: one, due to interference effects, with a decay constant (τ_D^{-1}) proportional to the particle diffusion coefficient and with an amplitude proportional to N^2 (N is the average particle concentration) and one, due to scattering volume occupation number fluctuations [Schaefer and Berne, Phys. Rev. Lett. (1972) 28, 475-477], with a decay constant (τ_N^{-1}) related to the diffusion time through the scattering volume and with an amplitude proportional to N (usually $\tau_N >> \tau_D$). The ratio of the two amplitudes is proportional to the absolute particle concentration, with a proportionality constant dependent on system optics which can be measured or computed. The average intensity also is proportional to particle concentration, but the proportionality depends on the particle scattering efficiency, which may be difficult to measure absolutely. However, LBFS may be used to calibrate the average scattered intensity for each type of particle. Using LBFS to obtain virus particle concentrations, we have determined the per virion Reverse Transcriptase activity for AMV and MuLV with the synthetic template poly rC-oligo dG in 0.1 M Mg^{++} for AMV and 0.01 M Mn^{++} for MuLV. GTP incorporation (p moles/virion/hour incubation) was 5.4×10^{-8} and 257×10^{-8} for MuLV and AMV respectively.

Supported by NCI Contract #NO1-CP-33226.

TH-PM-I4 SAMPLING STATISTICS IN SEARCHING FOR VIRUS PARTICLES IN HUMAN TUMORES. IMPROVEMENT USING AN AUTOMATED HIGH VOLTAGE ELECTRON MICROSCOPE WITH PATTERN RECOGNITION IMAGE PROCESSING. D.F. Parsons and D.A. Whaley*, Electron Optics Lab., Roswell Park Memorial Institute, Buffalo, N.Y. 14203.

Virus-like particles have been located only in a few human tumor tissues. Sampling statistics may have been inadequate in past searches for virus particles. A one year project using a 100KV EM (15,000X) with 35 micrographs per day, results in the examination of the equivalent of a single 30 μm cell. Thus past surveys are likely to be of limited value. A remedy is suggested involving improving the sampling of biopsy material and automation of a 1.2 MeV HVEM (being installed at N.Y.State Dept. of Health Labs. Albany). Optimum statistical procedures are used in sampling of the blocks and sampling of ribbons of sections. Using the HVEM the sections can be increased to 1 μm thickness giving a gain in volume of tissue of 11 times. (With image processing analysis of stereo-pairs the thickness can possibly be increased to 3 μm). Clusters of 1-3 μm sections will be placed on a slotted tape and scanned under computer control. A section is selected by use of beam transmission and it's detail assessed from the FFT spectrum. (The FFT will also control adjustment of the focusing and stigmator). A special 1000 line TV system will feed digitized picture data to a computer where round virus particles will be identified by a pattern recognition technique. If particles are present they are circled and the image is placed on tape. In an overnight work period of 15 hours, using the TV tube optimally with a prepare, expose and read cycle of 3.6 minutes, 250 micrographs will have been examined. Automation and thickness allow a minimum gain of 80 times in the volume of tissue examined compared to conventional electron microscopy.

TH-PM-I5 THE KINETICS OF VIRUS INDUCED CELL FUSION. S. Person, R. W. Knowles*, G. S. Read*, S. C. Warner* and V. C. Bond*, Department of Biophysics, The Pennsylvania State University, University Park, Pennsylvania 16802.

Two years ago we began a research project whose major goals were to identify the molecules and sequence of reactions responsible for causing virus-induced cell fusion. We chose to study cell fusion induced by Herpes Simplex Virus (HSV) because, although the wild type virus does not produce cell fusion, a number of reports indicated that wild type variants, possibly mutants, do cause fusion. We have isolated a number of these mutants, termed *syn* mutants, from a wild type strain of HSV type I, called KOS, and have begun to biochemically and genetically characterize the *syn* mutants following their infection of secondary cultures of human embryonic lung cells. We present here a simple quantitative assay for cell fusion obtained by using a Coulter counter to measure the change in number of small single cells as a function of time after infection. Following the onset of fusion there is an exponential decrease in the number of small single cells. Data obtained using the Coulter counter will be compared with the more conventional microscope assay. Using the former assay we will present data that compare a *syn* mutant with a wild type infection, as well as mutant infections at multiplicities of infections from 0.47 to 104. Finally we will present data to show that *syn* mutant-infected cells can fuse with either infected or uninfected neighboring cells.

TH-PM-I6 MINICELL PRODUCTION BY THYMIDINE REQUIRING STRAINS OF *HAEMOPHILUS INFLUENZAE*. Barbara Sedgwick* and J. K. Setlow (Intro. by M. Moody), Biology Department, Brookhaven National Laboratory, Upton, New York 11973.

Aminopterin resistant thymidine requiring strains (Rd *dThd*$^-$) of *H. influenzae* produce minicells. The ratio of minicells to cells increases during the stationary phase of the growth cycle. The greatest minicell yield (ratio 0.2) observed occurred after dense growth on Brain Heart Infusion agar. LB11, isolated after treatment of Rd *dThd*$^-$ with MMNG has an increased yield of minicells (ratio after growth on BHI agar, 1.0). The mutations involved in minicell production have been transferred into the wild type (Rd) by transformation. Strain Rdmc1 is thymidine requiring and has the same minicell yield as LB11. Spontaneous revertants of Rdmc1 to nonthymidine requirement do not produce minicells. Thymidine requirement and at least one other mutation are therefore necessary for a large yield of minicells. It was previously reported that competent cells of LB11 are superinducible for defective phage on exposure to transforming DNA. Rd *dThd*$^-$ and Rdmc1 are also superinducible under these conditions. The thymidine requirement therefore causes this superinducibility which does not appear to be dependent on the mutation(s) which enhance(s) the yield of minicells in Rdmc1 and LB11. This research was carried out in Oak Ridge National Laboratory under contract with the Union Carbide Corporation and at Brookhaven National Laboratory, both sponsored by the U. S. Atomic Energy Commission.

TH-PM-I7 GENETIC COMPOSITION OF TRANSFORMED CLONES OF HAEMOPHILUS INFLUENZAE. J. K. Setlow, Biology Department, Brookhaven National Laboratory, Upton, New York 11973.

Since transformation of H. influenzae takes place by insertion of a single strand of donor DNA into the recipient genome, one would expect the progeny of a transformed cell to be half transformants (if the cell contained only a single genome at the time of the recombination event) or one-quarter or one-eighth transformants if the cell contained 2 or 4 multiples of the genome. The clone could consist only of transformants if there were only one genome in the original transformed cell, and in addition either one of the first two daughter cells was inviable or there was enzymatic deletion of one or more bases opposite the inserted single strand region, followed by repair, with the inserted DNA as template. Fifty clones containing transformants have been analyzed following exposure of wild type or mutant (ATP-dependent nuclease deficient) competent cells to transforming DNA and nonselective plating. Two out of 18 mutant clones were purely transformants, but there were no pure wild type clones. These data may be explained in terms of the approximately 50% nonviability of the mutant cells. The fraction of cells in the 32 wild type clones which were transformed ranged from 0.65 down to 3×10^{-6}, with no evidence of grouping of the values. The results do not appear interpretable by the simple model given above, but rather suggest the possibility that the time at which donor DNA begins to replicate as part of the cell genome varies markedly in different transformation events. This research was carried out in the Oak Ridge National Laboratory sponsored by the U. S. Atomic Energy Commission under contract with the Union Carbide Corporation.

TH-PM-I8 D PERIODS IN SLOWLY GROWING BACTERIA AS DETERMINED BY RESIDUAL DIVISION. H. E. Kubitschek, Division of Biological and Medical Research, Argonne National Laboratory, Argonne, Illinois 60439.

Values of the D period between termination of chromosome replication and cell division were determined from measurements of residual cell division after exposure of slowly growing exponential phase cultures of Escherichia coli, strains B/r and K12 AB1157, and of Salmonella typhimurium 9557 to chloramphenicol. As tested up to generation times of four hours or longer, values of the D period were independent of growth rate for each strain: 26.1 ± 1.2 min for E. coli B/r, 23.7 ± 2.8 min for E. coli K12, and 13.3 ± 0.6 min for S. typhimurium. The result for E. coli B/r is in excellent agreement with the earlier value of 25 min obtained for the same strain by a nonselective technique. These results continue to support the possibility that D periods are invariant in exponentially growing bacteria.

This work supported by the U.S. Atomic Energy Commission.

TH-PM-I9 PARTIAL CHARACTERIZATION OF THE DNA ISOLATED FROM BOVINE SPERMATOZOA. Shyamali Sur* and Irwin Bendet. Department of Biophysics and Microbiology, University of Pittsburgh, Pittsburgh, Pennsylvania 15260.

Bovine sperm cells were treated with 0.2% pronase in 0.002M $CaCl_2$ to remove their tails and the heads were then fractionated in a preformed sucrose gradient. The latter were disrupted in 5M GuHCl, 0.28M β-mercaptoethanol, 0.5M tris, 0.005M EDTA at pH 8.5. The resulting viscous solution was centrifuged in 5M CsCl at 35000 rpm for 40 hours and fractions collected. Each was dialysed exhaustively against 10^{-2} standard saline citrate plus 10^{-5}M EDTA, and the DNA was recovered from those fractions having an $O.D._{260}/O.D._{230}$ = 2.1. U.V. sedimentation velocity experiments on this material showed a homogeneous boundary with $S_{w,20}$ = 21. Aliquots of the DNA were prepared for electron microscopy by a modified Kleinschmidt procedure. Most of the DNA appeared like rosettes having one or more "cores", through which the DNA strands pass many times giving rise to loops. The length of DNA associated with the rosettes was found to vary widely, occasionally exceeding 50 microns, but averaging approximately 6-8 microns per core. Preliminary experiments to determine the nature of the core indicate that treatment with SDS reduces the compactness of the structure. The effect of enzymes is also being investigated. It is suggested that the rosettes may be native substructures of the sperm nucleoprotein by which the DNA is bound into a compact structure.

TH-PM-I10 SIZE AND STRUCTURE OF A MAMMALIAN DNA DETERMINED BY SEDIMENTATION AND CONFIRMED BY VISCOELASTOMETRY. CHRISTOPHER S. LANGE. University of Rochester School of Medicine & Dentistry, Rochester, New York 14642.

Native DNA of L5178Y mouse leukemia cells has been measured by velocity sedimentation under conditions where, for this molecule, rotor speed dependence does not apply and was found to exist in units of 1.7 (1.0-2.6 as 95% F.L.)$\times 10^{10}$ daltons, which corresponds to the DNA content of 1/8th of the average chromatid. Measurement of this DNA in the Cartesian diver viscometer of Klotz & Zimm (J.Mol.Biol., 72, 779(1972)) yields two independent size estimates. The relaxation time yields an estimate of 1.3 (0.9-2.0 as 95%F.L.)$\times 10^{10}$ daltons and the recoil yields 481 (± 8%S.E.M.) such molecules per log phase cell which results in an estimate of 1.6 (1.2-2.5 as 95%F.L.) $\times 10^{10}$ daltons for this large DNA unit. Special gradients with an "enzyme layer" have been used to demonstrate that this DNA is composed of about 21 subunits of 8×10^{8} daltons each, linked together in tandem by disulphide containing protein linkages. Models for the organization of these subunits and linkages will be discussed. This paper is based on work performed under contract with the U.S.A.E.C. in the Department of Experimental Radiology (Contract No. AT(11-1)-3501) and at the University of Rochester Atomic Energy Project and has been assigned Report No. UR-3490-638. The author would like to acknowledge the help of Drs. E.H. Uhlenhopp & B.H. Zimm with the viscoelastometry, Ms. P. Mitchell with the sedimentation studies, and the support of an N.I.H. Research Career Development Award.

TH-PM-I11 STUDIES ON CONFORMATIONAL CHANGES IN CALF THYMUS CHROMATIN DURING TRANSCRIPTION. W.Wachsman, W.B.Rippon, and D.D.Anthony*, Depts of Pharmacology and Macromolecular Science, Case Western Reserve Univ, Cleveland, Ohio 44106

Interactions between proteins and DNA are believed to be significant in modulation of RNA synthesis. Effects of temperature and transcription were comparatively analysed for chromatin and DNA by circular dichroism in the spectral region between 310 and 250 nm. An increase in temperature to 45°C had no detectable effect on the spectral characteristics of chromatin. Addition of either ATP or E. coli RNA polymerase increased the ellipticity at 270 nm and 37°C. Combination of chromatin and enzyme plus either ATP or the 4 ribonucleotide triphosphates caused a further increase in ellipticity at 270 nm and 37°C, but not at 2°C. This increase was time-dependent and multiphasic. Similar studies with free DNA showed that the ellipticity at 270 nm was 18% greater at 37°C than at 2°C. The magnitude of this change was 7-fold greater than the initial change observed by the addition of enzyme and ATP to chromatin at 37°C. Addition of enzyme plus ATP to DNA caused an additional increase in the ellipticity at 37°C. Kinetic analysis at 270 nm and 37°C indicated that the change observed for DNA plus enzyme and ATP was also multiphasic. Correlative function studies were also done. Comparison of spectral data under conditions in which transcription occured and in which the rate of synthesis of poly A was modulated suggested that the spectral changes are due to both conformational changes in the template and product formation.
Supported by PHS. #5 T01 GM00661-12 (and 13) and Am.Cancer Soc. P-463 B

TH-PM-I12 NUCLEASE ACTION ON CHROMATIN: EVIDENCE FOR DISCRETE NUCLEOPROTEIN SUBUNITS. Randolph L. Rill.* (Int. by J. Herbert Taylor) Dept. of Chemistry, The Florida State University, Tallahassee, Florida 32306.

The time course of the fragmentation of chromatin from calf thymus, calf liver, rat liver, and chinese hamster ovary cells by a variety of nucleases has been examined by sedimentation of chromatin digests on linear (5-20%) sucrose gradients. All of the nucleases (DNase I, DNase II and micrococcal nuclease) act non-randomly. DNase II ultimately produces roughly equal amounts of acid-soluble oligonucleotides and 11S nucleoprotein particles which have a compact conformation and contain double-stranded DNA that is approximately 400Å or 120 base pairs long as measured by electron microscopic examination of deproteinized samples. Multiple units containing predominantly 800Å, 1200Å, and 1600Å lengths of DNA have been isolated from chromatin less extensively digested with DNase II, suggesting that the units are repeated in tandem along certain regions of chromatin fibrils. Limited micrococcal nuclease and DNase I digestion of chromatin produces a mixture of discrete nucleoprotein particles similar to those obtained with DNase II, but the final digestion product appears to contain fragments of the 11S particles as well as intact particles and acid soluble oligonucleotides. Subtle differences between the actions of DNase II and micrococcal nuclease may result from the ability of micrococcal nuclease to cleave within the 11S subunits. Complications of nuclease digestion experiments due to contaminating proteases will be discussed.

TH-PM-113 ORGANIZATION OF MAMMALIAN CHROMOSOMES INTERPRETED FROM RADIATION AND OTHER STUDIES. A. Cole, S. Robinson*, F. Shonka*, R. Datta*, and R. Chen*, Department of Physics, M.D. Anderson Hospital & Tumor Institute of The University of Texas System Cancer Center, Houston, Texas 77025.

A model for chromosome organization will be presented which is based on the variety of experimental results outlined here. Electron microscopic studies suggest that the mitotic chromatid contains about 64 DNA molecules of about 10^9 Daltons arranged in a quasi-parallel array which is collapsed when in a condensed configuration. Ultracentrifuge studies indicate common DNA sub-units of about 10^9 Daltons for native DNA and $0.5 \cdot 10^9$ Daltons for single strand DNA from interphase cells, interphase nuclei, mitotic cells, and mitotic chromosomes. Irradiation studies imply that there is one primary site per DNA sub-unit molecule which is very susceptible to radiation breakage which results in the subsequent release of DNA from a structure involving membrane or other components. Treatments with enzymes and other agents indicate that protein, RNA, or sulfhydryl linkages are not integrally involved in this structure. Multiple secondary sites, which constitute about 10% of the DNA mass, are less radiosensitive. The remaining DNA appears to be relatively radiation resistant. Studies with short penetration electron and alpha particle beams indicate that the primary and secondary sensitive sites are closely associated with the nuclear membrane of interphase cells. Studies on cell repair of double strand and single strand DNA breaks implicate different enzymatic systems involving one double strand repair complex and multiple single strand repair complexes per DNA sub-unit molecule.

Supported in part by AEC (DBER) Contract AT-(40-1)-2832.

TH-PM-114 STUDIES ON THE FRACTIONATION OF EUKARYOTIC DNA AT VERY HIGH MOLECULAR WEIGHT. D. W. Appleby and J. E. Hearst Department of Chemistry, University of California, Berkeley, California 94720.

In our studies of the distribution of DNA sedimentation coefficients present in the Kavenoff-Zimm lysate of D. melanogaster cells, we have found that it is possible to divide the molecules present into two groups: a fast group and a slow group. The two groups exhibit very different equilibrium density gradient profiles, the yield of satellites in the fast group being significantly lower than in the slow group. The minimum and maximum estimates of molecular weight are 0.3×10^9 and 7×10^9 g/mole.

Biophysical Journal vol. 15, 1975 206a

TH-PM-J1 CHANGES IN THE PROTEIN PROFILE OF HUMAN ERYTHROCYTE GHOST BY SONICATION. Mark W. Cowden and Chan Y. Jung. V.A. Hospital, Buffalo, N.Y. 14215.

Sonication of human RBC ghost (prepared by the method of Dodge et al) between 36-42° produced "mini ghost" (vesicles) 250-600 A in diameter. SDS gel electrophoresis demonstrated that membrane proteins of ghosts sonicated in 1/10 BSS did not differ significantly from those of nonsonicated ghosts. On the other hand, sonication of ghosts with the omition of divalent cations (Mg^{++} and Ca^{++}) from the 1/10 BSS (solution I), resulted in the disapearance of bands I, II and IIa (a minor band just below band II) and a partial loss of bands III, IV and V (band nomenclature after Fairbanks, Steck and Wallach, 1971). The presence of EDTA at 0.1 mM in solution I prevented the dissapearance of bands I and II. It is of interest that these proteins are the proteins that have been observed to dissapear from gel of ghosts treated with Ricinus communis lectin and a protein cross-linking agent (Ji and Nicolson, Proc. Nat. Acad. Sci. 71; 2212, 1974). Diffuse protein material is detected between the major bands II and III; IV and V; and just after band VI, however, the protein material found in these regions appear not to account for all the protein lost from the above mentioned bands. The SDS gel electrophoresis of extracted spectrin (1.0 mM Tris-HCl, 0.1 mM EDTA, pH 8.0 supernatent dialysed against solution I) indicated that spectrin dissapears from the SDS gels only when it is sonicated in a glass tube, but not when it is sonicated in a plastic (polystyrine or polyethylene) tube. Preliminary experiments indicated that sonicated ghosts just prior to lysis still retain glucose carrier activity intact. It is anticipated that these sonicated vesicles could be used to incorporate this function into cells difficient in this function. (Supported by funds from NIH and VACO).

TH-PM-J2 LABELING OF CELL SURFACE: A CHELATING AGENT FOR BINDING OF METAL IONS TO SURFACE PROTEINS OF RABBIT ERYTHROCYTE MEMBRANE. Karl J. Hwang and John D. Baldeschwieler*, Division of Chemistry and Chemical Engineering, California Institute of Technology, Pasadena, California 91125.

A bifunctional chelating reagent utilizing the covalent metal binding molecule 1-(p-benzenediazonium)-ethylene diamine-N,N,N',N'-tetraacetic acid, azo-phenyl-EDTA, has been synthesized. The complex of this compound with Indium-111, azo-phenyl-EDTA(In-111), cannot pass through the red blood cell membrane. When added to intact red blood cells, it combines covalently with the outer components of the rabbit erythrocyte membrane. Proteins with molecular size from 35,000 to 75,000 daltons are intensively labeled. Some proteins are free of label. Supported by NIH grant GM 21111-02.

TH-PM-J3 THE RELATIONSHIP BETWEEN PERMEATION OF AN ANIONIC PHOTOREACTIVE PROBE AND ITS BINDING TO RED BLOOD CELL MEMBRANE PROTEINS

Z.I. Cabantchik, T. Ostwald*, P.A. Knauf and A. Rothstein, Institute of Life Sciences, Hebrew University, Jerusalem, Israel, and Research Institute, Hospital for Sick Children, Toronto, Ontario, Canada.

(^{35}S) NAP-taurine(N-(4-azido-2-nitrophenyl)-2-amino ethyl sulfonate, developed by Staros & Richards (Biochemistry 13:2720,1974) as a photoreactive label for surface proteins of red blood cells, is found to interact with superficial membrane sites related to anion permeability. The penetration of the anionic probe through the membrane in the dark at 37°C is blocked by specific inhibitors of anion fluxes. Photoactivation of the probe restricted to the outer surface of cells (0°C) leads to a specific and irreversible inhibition of anion permeation (sulfate). The inhibitory sites are apparently those that also react with disulfonic stilbene derivatives, specific inhibitors of anion transport. The common sites are located in a membrane protein band (III) of apparent molecular weight 95,000 (SDS-acrylamide-gel electrophoresis). A 65,000 molecular weight segment of this protein which resists proteolytic treatment of cells contains most of the irreversibly bound probe. On the basis that NAP-taurine can be both a substrate of and an irreversible inhibitor of the anion transport system, it is concluded that the 95,000 m.w. protein is directly involved in anion transport. Supported by MRC (Canada) Grant No. 4665.

TH-PM-J4 INTERACTION BETWEEN PHLORETIN AND THE RED CELL MEMBRANE.

M.L. Jennings* and A.K. Solomon, Biophysical Laboratory, Harvard Medical School, Boston, Massachusetts 02115.

Phloretin binding to red cell components was examined at pH 6, where binding and inhibitory potency are maximal. Binding to intact red cells and to purified hemoglobin (Hb) are nonsaturable processes approximately equal in magnitude, which strongly suggests that most of the red cell binding may be ascribed to Hb. This conclusion is supported by the fact that Hb-free red cell ghosts can bind only about 10% as much phloretin as an equivalent number of red cells. Moreover, the concentration dependence of the binding in Hb-free ghosts reveals at least two saturable components. Phloretin binds with high affinity (K_{diss}=1.5μM) to about 3×10^6 sites per cell; it also binds with lower affinity (K_{diss}=50μM) to a second (6×10^7 per cell) set of sites. In sonicated total lipid extracts of red cell ghosts phloretin binding consists of a single, saturable component. Its affinity and total number of sites are identical to those of the low affinity binding process in ghosts. No high affinity binding of phloretin is exhibited by lipid extracts. Hence phloretin inhibition of glucose transport and anion exchange, which occur at 1-2μM phloretin, must result from direct interactions with membrane proteins. However, 100mM glucose does not detectably displace any of the high affinity binding. Since phloretin is thought to compete with glucose for transport sites, this implies that only a small fraction of the high affinity sites are associated with glucose transport. At concentrations about 20μM, phloretin exercises a number of generalized effects on membrane function. Since the bulk of the phloretin binding in this concentration range is with the lipid component of the membrane, it appears that the effect of phloretin at these higher concentrations is lipid mediated. Supported by USPHS grants 2TO1GM00782-16 and 5FO1GM48416-04.

Biophysical Journal vol. 15, 1975 **210a**

TH-PM-J5 SPECTRIN: A POSSIBLE PROTEIN COMPONENT OF THE GLUCOSE TRANSPORT SYSTEM IN THE HUMAN ERYTHROCYTE. S. J. Masiak* and P. G. LeFevre, Department of Physiology and Biophysics, Health Sciences Center, State University of New York at Stony Brook, Stony Brook, New York 11794.

Treatment of a 5% suspension of washed human erythrocytes with trypsin or α-chymotrypsin (5 mg/ml) for up to 4 hr has no effect on the carrier-mediated movement of glucose, as determined by the Ørskov method. However, when these proteolytic enzymes are enclosed within reconstituted cells upon reversal of hemolysis (2 min in 30 mM NaCl at room temperature), there is a progressive inhibition of glucose movement. This inhibition is prevented if the enzymes are boiled or pre-inhibited with soybean trypsin inhibitor before incorporation. Trypsin is about four times as effective as chymotrypsin in this action (e.g., 50% reduction in glucose exit rate within 45 min vs. 180 min, with enzymes at 0.5 mg/ml). These results strongly suggest that a protein located on the interior surface of the cell is involved in sugar transport. Therefore, at various time intervals after the incorporation of the proteases, these cell preparations were rehemolysed in the presence of a tenfold excess of soybean trypsin inhibitor and the dissolved membrane proteins separated electrophoretically on SDS-polyacrylamide gels. Only one major protein band (spectrin, known to reside at the inner membrane surface) showed a loss during the protease treatment; this loss paralleled the development of glucose transport inhibition. We accordingly propose that spectrin is involved in the glucose transport operation, in spite of recently reported evidence that it does not contribute to the binding of the potent transport inhibitor, cytochalasin B. The 90,000-MW band, reported to react specifically with an "affinity label" for this transport system, was not noticeably affected here. (Supported by NSF Grant BO-12685 and NIH Grant AM16821)

TH-PM-J6 ELASTIC BEHAVIOR OF SPECTRIN-PHOSPHOLIPID MEMBRANES. P.L. La Celle, Depts. Medicine, and Rad. Biol. & Biophys., Univ. of Rochester, Rochester, New York, 14642.

The human erythrocyte membrane appears to possess the properties of elasticity, and two dimensional incompressibility despite capacity for great unidirectional extensibility, and is isotropic. A lipid bilayer membrane containing intrinsic proteins would not be expected to confer the observed solid material properties, even if bending resistance is considered. Preliminary studies have indicated that addition of erythrocyte membrane protein to an oxidized cholesterol bilayer enhanced its strength and tended to confer elasticity. The current investigations attempted to define acquired characteristics of phospholipid bilayers formed from pure phospholipids when pure (crystallized) albumin, the water soluble erythrocyte proteins spectrin and Band 5, and F-actin and heavy meromyosin were placed in solution on one side of lipid bilayer. Membrane elasticity of the composite bilayer-adsorbed protein was compared to that of the original bilayer and normal erythroctye "ghost" membranes by measurement of extension ratio (λ) of membranes aspirated into 0.5 μm glass micropipettes in a microscope stage chamber as a function of deforming force. Pure lipid bilayers ruptured at forces <100 dynes/cm^2 at $\lambda \leq 1$; addition of albumin to final concentration of 10 mg/ml in the chamber on the side of membrane opposite the deforming micropipette reduced rupture rate and increased λ, as did spectrin in concentration of 1.5 mg/ml. F-actin, 3.12 mg/ml and heavy meromyosin 0.3 mg/ml had no effect. Phospholipid-spectrin "membranes" properties withstood forces up to 150 dynes/cm^2, and exhibited λ 0.7 to 1.2. These data suggest that spectrin may account for the elastic solid property of the normal erythrocyte membrane.

TH-PM-J7 POTASSIUM TRANSPORT AND Na-ATPase ACTIVITY IN SHEEP RETICULOCYTES P.B. Dunham and R. Blostein, Dept. of Biology, Syracuse Univ., Syracuse, N.Y. and Div. of Haematology, Royal Victoria Hospital, Montreal, Canada.

Active K transport and Na-ATPase were measured in red cells from LK and HK sheep made anemic by phlebotomy. Following density gradient separation of young from older red cells, the ouabain-sensitive K influx (^{42}K influx in 5 mM K) and membrane Na-ATPase (assayed at 0.2 μM ATP) were measured. Young cells, including reticulocytes, of both HK and LK sheep had higher maximal K influx and Na-ATPase than mature cells, i.e. K pump: 5-fold higher in HK and 10-fold higher in LK; Na-ATPase: 3-fold higher in HK and 30- to 40-fold higher in LK. In both types of immature cells and in HK cells, the pump was stimulated at low intracellular K (K_i) and was inhibited at higher (K_i), albeit to a relatively small extent. In contrast, LK mature cells were strongly inhibited by (K_i) at all concentrations of (K_i) tested. The kinetics of Na-ATPase of HK and LK reticulocytes resembled in one respect that of mature LK cells (strong K+- inhibition at 0.2 μM ATP), in other respects, HK mature cells (effect of [ATP] on K+- inhibition and oligomycin response). The results suggest that the two types of pump sites, HK- and LK-sites, co-exist in immature cells, but are apparent to different extents, depending upon the parameter measured i.e. although a particular test may indicate predominance of one type, another test may indicate predominance of the other type. This possibility is supported also by preliminary results showing that LK reticulocytes possess pump sites which, like LK-type pumps of mature LK cells, are stimulated by specific isoimmune anti-L antibody. Supported by grants from the MRC of Canada (MT-3876) and the NIH (AM 16196).

TH-PM-J8 MEASUREMENT OF THE KINETICS OF BICARBONATE TRANSPORT IN HUMAN ERYTHROCYTE SUSPENSIONS. E.I. Chow*, E.D. Crandall* and R.E. Forster, Department of Physiology, University of Pennsylvania, Phila., Pa., 19174.

The kinetics of bicarbonate transport across the human red cell membrane was studied by following the time course of extracellular pH in a stopped-flow rapid-reaction apparatus with a glass electrode measuring device during transfer of H^+ into the cell by the CO_2 hydration-dehydration cycle under conditions where the process was rate-limited by HCO_3^- flux across the membrane. These conditions were produced by rapidly mixing a suspension of red cells in saline containing carbonic anhydrase and 0.2 to 40 mM total CO_2 at pH 7.8, with a CO_2-free buffer solution at pH 6.8. The rate constant for the movement of HCO_3^- across the red cell membrane is 6.4 sec^{-1} at 37°C and 0.11 sec^{-1} at 2°C. The flux of bicarbonate increased linearly with the HCO_3^- concentration gradient across the red cell membrane at both 37° and 2°C, and decreased as transmembrane potential(V_i-V_o) increased (produced by changing extracellular Cl^- concentration) from -10mv to +48mv. The permeability of the red cell membrane to HCO_3^- calculated according to the constant field passive diffusion theory is 2.4 x 10^{-4} cm/sec at 37°C and 3.8 x 10^{-6} cm/sec at 2°C. An Arrhenius plot of the rate constants indicates that the Q_{10} for HCO_3 transport is strongly dependent on temperature, being about 1.8 between 12° and 42°C and about 7 between 2° and 12°C. The former Q_{10} corresponds to an activation energy of 11 Kcal/mole and the latter to an activation energy of 30 Kcal/mole. These data agree well with previously reported Q_{10} of 1.2-1.5 between 10° and 40°C (Luckner, Pflügers Arch., 250:303, 1948) and Q_{10} of 8 between 0° and 10°C (Dalmark, & Wieth, J. Physiol., 224:583, 1972). These results suggest that different processes dominate Cl^--HCO_3^- exchange at low versus physiological temperatures.

Biophysical Journal vol. 15, 1975 **212a**

TH-PM-J9 MEMBRANE RESTRICTED DIFFUSION OF WATER IN PACKED HUMAN RED CELLS. Kenneth R. Foster and Edward D. Finch, Neurobiology Department, Armed Forces Radiobiology Research Institute, and Biophysics Division, Naval Medical Research Institute, Bethesda, Maryland 20014.

We have used the spin-echo pulsed field gradient NMR technique to measure, as a function of diffusion time interval, water diffusion through packed human red cells. For time intervals between 20 and 50 msec, we observe two distinct water components with different diffusion constants. The faster component has a diffusion constant approximately one-third that of bulk water and an activation energy of about 6 kcal/mole. The slower component has a diffusion coefficient of about 7 percent that of bulk water and an activation energy near 12 kcal/mole. At 20°C, the fast component comprises about 60 percent of the observed water. Treating the cells with p-chloromercuribenzoate reduces the size of this fraction. In the time domain of our experiment the cell membrane, rather than bulk diffusion, is the rate limiting barrier to water movement. The fast and slow components which we have observed are tentatively identified with diffusion through water filled pores and through membrane lipids, respectively.

TH-PM-J10 PERMEABILITY OF HUMAN ERYTHROCYTES TO $H_2{}^{17}O$. M. Shporer* and M.M. Civan, Isotopes Dept., Weizmann Institute of Science, Rehovoth, Israel, and Depts. of Physiology and Medicine, University of Pennsylvania School of Medicine, Philadelphia, Pa. 19174.

Water permeability of human erythrocyte membranes has been studied by measurements of: efflux of tritiated water, light scattering during hydro-osmotically-induced volume changes, and the longitudinal relaxation time (T_1) of water protons in the presence of extracellular Mn^{++}. The first two techniques are subject to significant experimental error because of the needs for rapid mixing and measurement over periods of msec; results obtained by the third technique might reflect permeability changes induced by Mn^{++}. Pulsed NMR measurements of ^{17}O from $H_2{}^{17}O$ in cell suspensions circumvent these problems. After incubation in a saline solution enriched with 10-18% $H_2{}^{17}O$, T_1 of the ^{17}O was determined separately in samples of packed cells, supernatant and suspensions. The longitudinal relaxation in cell suspensions was non-exponential, reflecting water exchange across the cell membranes, as well as relaxation processes inside and outside the cell. The T_1 of intracellular ^{17}O was 4-5 times shorter than in the supernatant, similar to the enhancement of proton relaxation by hemoglobin in erythrocytes and in free solution at the frequency applied (8.13 MHz). This datum is consistent with the thesis that hemoglobin modifies the NMR relaxation behavior of water inside cells and in free solution in the same way. The rate constant (k_x) for water exchange was calculated to be 60 and 107 sec^{-1} at 25 and at 37°C, respectively. The apparent activation energy for k_x over the temperature range 23-37°C was 8.7 ± 1.0 kcal/mole. (Supported in part by Res. Grants from the NSF (GB-40040X) and the US-Israel Binational Sci. Found. (No. 366). MMC is an Established Investigator of the Am. Heart Assoc.)

TH-PM-J11 PYRENE FLUORESCENCE AS A PROBE OF ERYTHROCYTE MEMBRANE FLUIDITY. M. Dembo*, V. Glushko and M. Sonenberg. Memorial Sloan-Kettering Cancer Center, New York, N. Y. 10021

Excited pyrene monomers react with ground state monomers to form excited state dimers or excimers, undergoing a 100 nm red shift in fluorescence emission. The rate of excimer formation is a diffusion controlled collision process that is related to the viscosity of the environment by a special case of the Einstein-Smoluchowski diffusion theory. As observed by J. B. Birks, the excimer nanosecond fluorescence response function can be characterized by the difference of two exponentials with decay times τ_1 and τ_2. The initial rate of increase in the response function equals the product of the diffusion controlled rate of excimer formation and other, temperature independent, factors. Therefore it is possible to measure changes in the fluidity of the excimer microenvironment as a function of temperature without having to identify the thermal effect on each rate constant. The hydrophobic compartment of erythrocyte membranes readily incorporates pyrene from 0.025 osmolar tris pH 7.4 buffer, with a partition coefficient in excess of two orders of magnitude. A significant amount of pyrene must be incorporated as excimer formation is negligible below an effective mM concentration. The kinetics of excimer formation in nitrogen flushed erythrocyte ghosts were studied by both quantum yield and fluorescence lifetime measurements. Increasing the temperature from 10° to 50° decreased the decay parameters τ_1 and τ_2 from 220 to 100 nsec and from 35 to 25 nsec, respectively. Over the same temperature range, the rates of excimer formation gave a linear Arrehenius plot yielding an activation energy of 6 kcal for the diffusion constant. This indicates that erythrocyte membranes provide a fluid, though viscous, environment for pyrene. (NIH CA-08748,-16889; Am. Cancer Soc. BC-119).

TH-PM-J12 TEMPERATURE JUMP RELAXATION STUDY OF HUMAN ERYTHROCYTES. T. Y. Tsong and E. Kingsley*, Department of Physiological Chemistry, The Johns Hopkins University School of Medicine, Baltimore, Maryland 21205.

Complex transient signals were observed in an isotonic suspension of human erythrocytes when the suspension was subjected to a rapid temperature jump (heating time of 2 μsec). The signals reflect a fast biphasic decrease in turbidity (with two relaxation times: τ_1 = 20 μsec and τ_2 = 5 msec) followed by a slower restoration of turbidity to nearly its initial value (τ_3 = 0.5 sec). These turbidity changes of the suspension are consistent with a swelling of the cells followed by a shrinking. The swelling may be caused by a temperature jump-induced transport of water into the cells and the shrinking may be a result of membrane rupture after excess swelling. [^{3}H]glucose-trapping experiments, hemolysis measurements and light microscope examinations all agree with these assumptions. The hemolysis of the red cell required a temperature jump of 0.5°. The water transport occurs at a much smaller perturbation level, around 0.02°. When the osmolarity of the suspensions was varied, the maximum water transport occurred at the isotonic condition. The signals of the turbidity increase were proportional to the fraction of unlysed cells in the suspensions. In the isotonic condition the apparent activation energies are, respectively, 8.4, 12.0 and 11.8 kcal/mole for τ_1, τ_2 and τ_3 reactions. The phenomena of the water transport induced by the temperature jump may be understood by the theory of thermal osmosis (Spanner, Symp. Soc. Exptl. Biol., 8, 76, 1954). Slow heating of the suspension shows no such effects. This work was supported by NSF Grant GB-38374 and NIH Institutional Grant FR-5378.

TH-PM-J13 ULTRASONIC MEASUREMENT OF MOLECULAR RELAXATION IN RED CELL MEMBRANES. John W. Dooley* (Intr. by John Sachs), Brooklyn College of the City University of New York, Brooklyn, New York 11210.

Ultrasonic attenuation measurements constitute a powerful probe for molecular conformation changes. The coupling of sound to a molecule can be enhanced by imbedding the molecule in a membrane rather than suspending it in a bulk solution. Measurements on human red cells and red cell ghosts in the frequency range 100 MHz to 300 MHz and Temperature range 5 to 30 degrees C show several relaxation peaks in the attenuation, two of which are reported here. The observed nanosecond relaxation times are fast for overall biological processes, but typical for individual molecular relaxations. The peaks appear to follow an Arrhenius law, with activation energy between 20 and 24 kCal/mole. The peaks are reproducible for samples from different donors, for various preparation techniques, and for varying values of pH. However, the strength and resolution of the peaks are enhanced at some ultrasonic frequencies. Such frequency dependence is predicted by a simple model for a spherical ghost.

TH-PM-J14 TRANSITORY POSTNATAL HEMOLYSIS OF CALF CELLS BY AMINO ACIDS. Hyun Dju Kim. Department of Physiology, College of Medicine, University of Arizona, Tucson, Arizona 85724, U.S.A.

Among amino acids which can be solublized to give 300 mM at near physiological pH, Histidine, Proline, Hydroxyproline, Valine, Threonine, Serine Glutamine and Glycine causes hemolysis of the newborn calf but not the adult cow red cells. The 3% calf red cell suspension in 300 mM Histidine undergoes a complete hemolysis within 25 min at 38°C. This lytic process is accentuated by the increase in pH values from 6.5 to 8.0 and also by the increase in temperature with an activation energy of 19 KCal/mol. At 5 mM Histidine medium, calf cells exhibited a higher influx rate (0.66 μM/ml Rbc x hr) than the adult cow cell (0.36 μM/ml Rbc x hr). At 300 mM Histidine, there was an instantaneous uptake and/or binding amounting to 19.7 ± 2.9 (S.E.) μM/ml Rbc in the calf and 8.51 ± 3.36 (S.E.) μM/ml Rbc in cow cells with concomitant efflux of cations. Histidine induced hemolysis takes place unaccompanied by the cell swelling even though calf cells can reach the critical hemolyte volume of 1.25 under a variety of conditions. Hemolysis induced by Histidine decreases substantially when a calf reached two months of age at which time the red cells containing the fetal hemoglobin are virtually depleted. The results obtained during this neonatal period on the hemoglobin typings revealed that those cells resistant to Histidine hemolysis almost invariably contain the adult type hemoglobin suggesting a selective, specific action of the amino acids on the fetal cells. Although the exact molecular mechanism for the hemolysis is not known, this provides a simple useful means of acquiring one cell type in the hetereogenous neonatal cell populations. Supported by NIH Grant AM-17723, USPHS GRS Grant to Univ. of Arizona and Southern Arizona Heart grant.

TH-PM-K1 ALTERATION OF ACHOLEPLASMA MEMBRANE SURFACE ORGANIZATION BY LIPID PHASE CHANGES. B.A. Wallace*, F.M. Richards and D.M. Engelman, Dept. of MB&B, Box 1937 Yale Station, New Haven, Ct. 06520.

The distribution of non-lipid surface sites on Acholeplasma laidlawii membranes was investigated as a function of the physical state of the membrane lipids. Isolated membrane ghosts were labeled with biotinyl-N-hydroxysuccinimide ester, which does not interact with the membrane lipids. Reaction sites in the plane of the membrane were visualized for electron miscroscopy by treatment with crosslinked Ferritin-Avidin conjugate. Myristic, oleic and stearic acid-supplemented membranes were labeled at temperatures above and below their phase transition temperatures. It was found that sites in membranes labeled below the phase transition temperature are relatively dispursed over the membrane surface. In contrast, in those membranes which were labeled above their phase transition temperature patches of low label concentration appear. Furthermore, the aggregation was shown to be reversible: membranes labeled under patch forming conditions (above phase transition temperature) and subsequently incubated at a temperature below the phase transition exhibit a random distribution of sites equivalent to that seen in membranes labeled under dispersing conditions (below phase transition). These results suggest that a temperature-induced change in the physical state of membrane lipids can induce a change in the distribution of non-lipid membrane surface sites in an unexpected fashion, since the changes we observe are opposite to the behavior of freeze-fracture particles observed by others on the inner fracture faces of Acholeplasma membranes. Supported by grants from the N.I.H. and N.S.F.

TH-PM-K2 LECTIN-RECEPTOR INTERACTIONS IN LIPOSOMES. W. R. Redwood and V. K. Jansons*, Departments of Biochemistry and Microbiology, New Jersey Medical School, Newark, New Jersey 07103

The interaction between purified wheat germ agglutinin (WGA) and a WGA receptor incorporated into phospholipid vesicles was studied by following the changes in the 90° light scattering of the suspensions. The major sialoglycoprotein of dog erythrocyte membranes, isolated by the lithium diiodosalicyclate procedure, was incorporated into phosphatidylcholine vesicles by injecting an ethanolic solution of the purified phospholipid into an aqueous solution of the glycoprotein. Free glycoprotein was removed by ultrafiltration. Addition of the WGA to the glycoprotein-liposomes suspensions resulted in a significantly larger increase in light scattering than observed in the WGA-phosphatidylcholine vesicle suspensions without the glycoprotein. The light scattering titration curve displayed saturation at high WGA concentration (5×10^{-7} M) and was sigmoidal at lower WGA concentrations. The differential increase in light scattering upon the addition of the WGA was inhibited by the prior addition of N-acetyl-D-glucosamine to the glycoprotein-liposome suspensions. The degree of inhibition depended on the hapten concentration; 100% inhibition was observed at 5×10^{-2} M N-acetyl-D-glucosamine. In contrast, N-acetyl-D-galactosamine had little effect on the interaction at this concentration. Below pH 2.8, no lectin-receptor reaction was observed in the model system. Furthermore, glycoprotein-liposomes which had been pre-treated with neuraminidase displayed markedly lower reactivity with WGA. The characteristics of the glycoprotein-liposome interaction with WGA are reminiscent of cell agglutination reactions with lectins. The glycoprotein-liposome system may, therefore, provide a suitable model system to study cell agglutination reactions. (Supported by NIH Grant GM-18697 and ACS Grant IN-92C).

TH-PM-K3 KINETICS OF A Ca^{2+}-TRIGGERED MEMBRANE AGGREGATION REACTION IN PHOSPHOLIPID VESICLES. Jeffry Lansman* and Duncan H. Haynes, Department of Pharmacology, University of Miami Medical School, Miami, Florida 33152

Ca^{2+} and other divalent cations (M^{2+}) can trigger aggregation of phospholipid vesicles containing phosphatidic acid (PA) and phosphatidyl serine (PS). The reaction occurs at Ca^{2+} concentrations greater than 1 mM, is accompanied by an increase in light scattering, and proceeds as a "polymerization" reaction eventually forming such high aggregates that the vesicles precipitate. The initial reaction, dimerization, was studied with the stopped-flow technique. Dimerization resulted in a doubling of light scattering and occurred with a time constant ($t_{1/2}$) of ca. 0.5 sec. Analysis of the dependence of reaction amplitude and $t_{1/2}$ on the concentrations of vesicles and Ca^{2+} show that the Ca^{2+} binding is fast and that the dimerization proceeds according to:

$$2\ (\text{vesicle}\cdot n\text{Ca}^{2+}) \underset{k_{-1}}{\overset{k_1}{\rightleftharpoons}} \text{encounter complex} \underset{k_{-2}}{\overset{k_2}{\rightleftharpoons}} \text{stable complex}$$

and that the stable complex is effected by Ca^{2+}-mediated salt bridges between the two membranes. The values of the rate constants are insensitive to the choice of M^{2+} or negatively-charged lipid (PA or PS). Analysis for PA give: $n=0.5\ M^{2+}/PA$; $k_1=6.8\times10^9\ M^{-1}\ sec^{-1}$; $k_{-1}=(0.17\text{-}1.3)\times10^6\ sec^{-1}$; $k_2=(1.0\text{-}1.9)\times10^3\ M^{-1}\ sec^{-1}$. This means that ca. 200 collisions are required to produce a stable vesicle dimer and that the rate-limiting step is the transformation of the encounter complex into a stable complex, requiring 0.5-1.0 msec. This result is discussed in terms of the statistics of distribution and the rate of redistribution of Ca^{2+}-occupied polar head groups on the membrane surfaces. The results are applied to Ca^{2+}-induced fusion of biological membranes.

TH-PM-K4 EFFECT OF IONS ON THE PHOSPHATIDYLCHOLINE LAYER STRUCTURE AS INDICATED BY RAMAN SPECTROSCOPY‡ L.J.Lis* and J.W.Kauffman, Department of Materials Science, and D.F.Shriver* Department of Chemistry, Northwestern University, Evanston, Illinois.

The interaction of various inorganic ions with the phosphatidylcholine lamellar structure was investigated using Raman spectroscopy. The monopositive and mono- and dinegative ions studied at 1M concentration have little effect on the lipid Raman spectrum, while dipositive ions, especially Ca^{2+} and Cd^{2+}, show an increase in the lipid hydrocarbon trans C-C vibration and the lipid head group C-N stretch. Evidence will be presented which indicates that cadmium halide complexes and not the cadmium ion produce the largest changes in the spectra. The effect of Ca^{2+} and Cd-halide complexes on the lipid molecular motions above and below the lipid liquid crystalline phase transition will be discussed. These results indicate that the ion-lipid interactions are highly specific. The triiodide ion is the one anion which has a large influence on the amount of lipid cis C-C conformers. This result is mainly due to this anion's penetration of the lipid lamellae.

‡ Supported in part by the Office of Naval Research.

TH-PM-K5 INFLUENCE OF ACETONE ON SURFACE PROPERTIES OF RAT LUNG. R. A. Rhoades and M. L. Eskew.* The Pennsylvania State University, University Park, Pa. 16802. Alveolar stability in the mammalian lung depends, in part, on the surface-active material (surfactant) lining the alveoli. The present study examined the effect of acetone in vitro on surface properties of lung washes obtained from male Wistar rats averaging 350g. Surfactant was collected in Krebs-Henseleit bicarbonate buffer (KHB) from each set of lungs (N=6) and was then divided into two 25ml aliquots. To one aliquot, 30µl of acetone was added yielding a concentration of 16.3 mmoles/liter, and to the other one was added 30µl of KHB. Surface properties were assessed by measuring maximum surface tension (γmax), minimum surface tension (γmin) and stability index ($\bar{S}$) on a modified Wilhelmy balance. The addition of acetone resulted in a significant ($P<0.05$) 25% increase in γmin, indicating decrease of surface-active properties. Differences were also observed in $\bar{S}$, but these were not significant statistically ($P>0.05$) from controls. These data indicate that alteration of lung surfactant may serve as an underlying mechanism for pulmonary dysfunction associated with uncontrolled diabetes and exposure to acetone vapors.

TH-PM-K6 EFFECT OF DIET ON THE PHYSICAL PROPERTIES AND CHEMICAL COMPOSITION OF HUMAN PLASMA LIPOPROTEINS. J.D. Morrisett, R. Segura*, O.D. Taunton*, H.J. Pownall*, R.L. Jackson*, and A.M. Gotto, Baylor College of Medicine and The Methodist Hospital, Houston, Texas 77025.

The effects of dietary saturated (S) versus polyunsaturated (P) lipids on the structure and composition of human plasma lipoproteins has been studied. For two weeks four normal male subjects were fed an isocaloric diet containing 40% lipid which had a P:S ratio of 0.25 (diet S). After two weeks on an ad libidum diet (diet AL), these subjects were fed a diet similar to diet S except the P:S ratio was changed to 4.0 (diet P). The proportion of linoleic acid in the phospholipids, cholesteryl esters, and triglycerides of very low-, low-, and high density lipoproteins (VLDL, LDL, and HDL) was greater with diet P than with diet S. This effect was accompanied by a compensating lesser (greater) proportion of the more saturated fatty acids on diet P (S). The fluidity (f) of the lipoproteins was measured as a function of temperature (0-70°) by EPR using a small amphipathic spin label (TEMPO) and a spin-labeled fatty acid (12-DS), and by fluorescence using pyrene. On both diets S and P, the order of lipid fluidity was VLDL > LDL > HDL. Plots of log f vs 1/T gave straight lines exhibiting 1 abrupt slope change with HDL, 2 with LDL, and 2 with VLDL. The temperatures at which these changes occurred were:

	Diet S	Diet AL	Diet P
HDL	38-43	27-36	20-23
LDL	30-34, 48-53	28-32, 47-50	25-30, 41-45
VLDL	22-26, 38-43	22-25, 37-49	21-28, 40-50

These results demonstrate the direct effect of dietary lipid on the fatty acid composition of all 3 classes of lipoproteins and on the thermotropic properties of HDL and LDL. Supp'd by NIH 71-2156, RR-00350, and HL-14194.

TH-PM-K7 PHOSPHOLIPID SYNTHESIS DURING BACTERIOPHAGE φ6 INFECTION. J.A. Sands and R. A. Lowlicht*, Lehigh University, Bethlehem, Pa. 18015

Bacteriophage φ6 consists of a polyhedral ribonucleoprotein core and a lipid-containing envelope. The phospholipid composition of the φ6 envelope differs significantly from that of the host bacterium, Pseudomonas phaseolicola. Specifically, phosphatidylglycerol (PG) is the most prevalent phospholipid in the virus, whereas phosphatidylethanolamine (PE) is most prevalent in the host cell membranes. Pulse label experiments with $^{32}PO_4$ indicate that cellular phospholipid synthesis is altered during φ6 infection. Prior to and during the first half of the infectious cycle, PE synthesis predominates. Late in virus infection, however, the relative level of PG synthesis increases significantly. The quantitative details of these results will be discussed in terms of a general model for the φ6 envelope formation process.

Supported by grant BMS74-05587 from the National Science Foundation.

TH-PM-K8 ISOLATION AND CHARACTERIZATION OF A WATER SOLUBLE MEMBRANE PROTEIN FROM SUCKLING RAT ILEUM. E.R. Jakoi*, G. Zampighi*, and J.D. Robertson, Department of Anatomy, Duke University Durham, North Carolina 27710.

The ileal epithelium of suckling rat pups exhibits a specialized endocytic complex consisting of a tubular membrane network beneath the microvilli and a supranuclear vacuole. The endocytic membranes are covered by an ordered array of particles, 7.5 nm in diameter, with center-to-center spacing of 14.5 nm. In order to determine the structure-function relationships of these particles, endocytic membranes were isolated from the scrappings of the ileal epithelium by differential flotation. Subsequently the particles were liberated from the membrane by 10 mM $CaCl_2$ followed by dialysis against 0.5 mM EGTA. The dialysate was further resolved into two protein components by chromatography on a Sephadex G200 column. The purity of each protein peak was affirmed by electrophoresis on 7.5% polyacrylamide gels. It was established that the 7.5 nm diameter particles are n-acetylglucosaminidase, an enzyme capable of digesting some components of milk. The second protein component in 5mM $CaCl_2$ polymerized into a fiber 3nm in diameter. This protein after release from the membrane was in both a monomer and a decorated fiber form. The decorated fiber may be associated with lipid since differential flotation experiments showed it equilibrated with a density of 1.084. Furthermore these decorated fibers, when released from the membrane, were associated with n-acetylglucosaminidase activity. In the presence of 5 mM $CaCl_2$ plus 4 μM $BaCl_2$ the decorated fibers reassociated in a two dimensional paracrystal which approximated the lattice originally observed on the membrane. Thus the array of particles seen in the electron microscope is comprised of n-acetylglucosaminidase attached to the membrane via a protein capable of polymerizing into fibers.

TH-PM-K9 A STUDY OF THE PROTEINS OF FROG HEART CELL PLASMA MEMBRANE. Donald D. Doyle*, Thomas Y.C. Ting* and Lloyd Barr, Dept. of Physiology and Biophysics, University of Illinois, Urbana, Illinois 61801.

In order to begin the characterization of the role of membrane proteins in the permeability changes during the generation of action potentials we have undertaken the fractionation and characterization of the polypeptides and certain proteins of the plasma membrane of the amphibian cardiac muscle cell. Previously, we have shown that a highly enriched vesicular preparation of this membrane can be isolated (Barr, et al. BBA345:336, 1974). We have used the Weber-Osborn SDS acrylamide gel system to separate and identify the polypeptide constituents of various preparations. We have identified 30 bands in our SDS electrophoresis gels of whole plasma membranes using Coomassie Blue staining. In corresponding gels stained with PAS reagent we have identified 7 polypeptide bands, so far. The polypeptides of this membrane are difficult to dissolve and tend to aggregate. Treatment of the plasma membrane vesicles with 0.5 mM EDTA "solubilizes" about 20-50% of the membrane protein in 72 hours. "Solubilized" proteins are defined as those not pelleted by a 90 minute centrifugation at 100,000 G. This "soluble" protein gave bands on buffered (non SDS) acrylamide electrophoresis gels. One of these bands has 5'-nucleotidase activity. A fraction of the "soluble" protein obtained by Sephadex chromatography showed a strong affinity for TTX. The polypeptide composition of the "soluble" protein is quite similar to that of the whole membrane.

TH-PM-K10 DEVELOPMENTALLY RELATED EXPRESSION OF A PLASMA-MEMBRANE ASSOCIATED CARBOHYDRATE-BINDING PROTEIN IN DICTYOSTELIUM DISCOIDEUM. C.-H. Siu*, R.A. Lerner, R.A. Firtel*, W.F. Loomis, Jr.*, Department of Immunopathology, Scripps Clinic and Research Foundation and Department of Biology, U.C.S.D., La Jolla, California 92037.

The cellular slime mold Dictyostelium discoideum can undergo synchronous development and is an excellent organism for the study of cell-cell interactions. By selective radioiodination of the plasma membrane, we found that the expression of a number of surface proteins was developmentally regulated. Such proteins obviously offer interesting possibilities for studying the molecular basis of developmentally regulated cell surface interactions. We show here that the carbohydrate-binding protein (CBP) described by Rosen et al (PNAS 1973, 70:2554) is localized on the outer surface of the plasma membrane and is one of the proteins differentially expressed at this site during development. CBP was not detected on the cell surface of A3 strain amoebae grown on Klebsiella aerogenes, but began to appear in increasing amounts at 5, 7 and 9 hours after starvation. A number of pleiotropic non-cohesive mutants (coh$^-$) were isolated. CBP was absent from the cell surface of coh$^-$-3 and coh$^-$-4 and was present only in minute amounts in coh$^-$-5. A ts-coh$^-$ mutant which failed to agglutinate SRBC at the non-permissive temperature had CBP on the cell surface, implicating a possible defect in the carbohydrate-binding portion of the molecule. In toto, these studies suggest a role for the CBP in cellular cohesion and subsequent development.

TH-PM-K11 CONTRAST IN UNSTAINED SECTIONS. L. Brandes‡ M. Pear*and F.P. Ottensmeyer (Intr. by J.W.Hunt), Ontario Cancer Institute, 500 Sherbourne St., Toronto, Ontario, Canada M4X 1K9.

Resolution in bright field electron micrographs of stained sections is primarily determined by heavy atom clusters required for contrast and visibility of the biological structure. Omission of heavy metal stains results in loss of visibility. For unstained specimens other than sections great success in overcoming the contrast problem has been obtained by the use of dark field electron microscopy. In all of these cases, be they visualization of atoms or macromolecules, the specimen was always supported by a thin film, and contrast could be enhanced by making the film thinner. For sections, however, one has to rely entirely on the intrinsic electron density differences between specimens and embedding media, since thinning the section proportionately removes biological material also. For thick sections, stained or unstained, dark field provided only drawbacks, multiple scattering and energy losses in scattering resulting in low resolution images of poor or no contrast. The use of very thin sections, however, indicated that the dark field technique could increase the visibility of structures to the degree that heavy metals could be completely omitted from the preparation. Resolution in sections now appears to be limited only by chromatic aberration, and ultimately radiation damage.

TH-PM-L1 ELECTROPHOTOLUMINESCENCE OF CHLROPLASTS.

James Ellenson and Kenneth Sauer, Dept. of Biology, Harvard University; Dept. of Chemistry and Laboratory of Chemical Biodynamics, U. C. Berkeley.

Pre-illuminated spinach chloroplasts have been perturbed with sub-millisecond and millisecond length DC electric field pulses. A brilliant flash of stimulated emission (electrophotoluminescence, or EPL) having the spectral characteristics of chlorophyll fluorescence occurs during the perturbation. Studies have been made to try to elucidate the molecular events associated with the emission and the relation it bears to photosynthetic electron transport.

During an electric field pulse the initial EPL emission is characterized by a rise having a short induction period followed by a complex decay from the maximum emission level. This latter decay is composed of two main components. One, the "R" component, has a faster decay time than the second, or "S" component. Termination of a single field pulse results in a decay of emission which is composed of two exponential decays having $t_{\frac{1}{2}}$'s of 15± 2 and 38± 3 μsec. Evidence shows that these perturbation relaxation decays are characteristic of the R and S components, respectively. Besides their difference in perturbation relaxation kinetics, the R and S components also differ in their decay of emission capacity during the dark, their intensity dependence on field strength and susceptibility to treatment with the ionophore gramicidin D.

A sequence of two pulses produces strikingly different emission patterns depending on whether the second pulse is of the same or reversed polarity compared to the first. The nature of these results and other properties of EPL emission are explained in terms of the electrostatic properties of a theoretical thylakoid model.

TH-PM-L2 ENERGY TRANSFER IN THE PHOTOCHEMICAL APPARATUS OF CHLOROPLASTS.

W. L. Butler and M. Kitajima*, Department of Biology, University of California, San Diego, La Jolla, California 92037.

A model of the photochemical apparatus of chloroplasts is presented in the form of Photosystem I and Photosystem II complexes (each containing antenna chlorophyll, Chl a_I or Chl a_{II}, and their respective reaction centers) separated by a light-harvesting chlorophyll, Chl LH, which can transfer excitation energy to either of the two photosystem complexes. The model is also presented in the form of equations (based on the rate constants to depopulate the excited chlorophyll molecules) which predict, and account for, the known fluorescence yield changes of chloroplasts. The equations include a specific rate constant term, $k_{T(II\rightarrow I)}$, for energy transfer between Photosystem II and Photosystem I so that the equations may be used to analyze energy transfer within the photochemical apparatus as well. Photosystem I shows no fluorescence yield changes related to its own photochemical activity; the fluorescence of variable yield, F_V, emanating from Photosystem I is due to energy transfer from Photosystem II. Measurements of fluorescence induction curves at 690 and 730 nm were made at -196°C on chloroplasts frozen in the absence and presence of 5 mM Mg^{2+}. The absence of Mg^{2+} caused a marked decrease of F_V at 690 nm with only a small decrease of the initial F_o level of fluorescence. In fluorescence at 730 nm, the absence of Mg^{2+} had a very little effect on the extent of F_V but caused a marked increase of F_o. The analysis of the data within the context of the model indicates that the yield of energy transfer $\varphi_{T(II\rightarrow I)}$, and the fraction of the energy absorbed initially by Photosystem I are greater in the absence of Mg^{2+}.

TH-PM-L3 FLUORESCENT KINETICS OF CHLOROPHYLL IN PHOTOSYSTEM I AND PHOTOSYSTEM II ENRICHED FRACTIONS OF SPINACH. W. Yu*, R.R. Alfano*, Physics Department, City College of New York, NY, NY 10031, and M. Seibert, GTE Laboratories, Waltham, Mass. 02154.

The fluorescent emission kinetics of Photosystem I (PSI) and Photosystem II (PSII) fractions of spinach have been studied on a picosecond time scale. Fractions were prepared by either the digitonin (PSI) or French Press (PSI and PSII) methods, and the fluorescence was measured using picosecond laser pulses and an optical Kerr gate. In both fractions the fluorescent risetime was $\leq$ 5ps. The fluorescent lifetimes (τ) for PSI and PSII fractions were 60±10 ps and 200±20 ps, respectively. In each case the fluorescence decayed exponentially. These measurements were determined in the region where the total fluorescence was linearly proportional to the excitation flux. The extrapolated intercept at zero excitation was zero in both fractions. Using the above measured τ's and the radiative τ of 15.2 ns for Chl, one can calculate quantum yields of 0.004 for PSI and 0.013 for PSII which are in good agreement with the measured values (1). Previously, 2 fluorescent components--1 with a short and 1 with a long τ--were observed in the fluorescent kinetics of chloroplasts (2). These components were interpreted as arising from PSI and PSII. Present work supports these assertions. The algebraic sum of the fluorescent kinetics observed in this study for PSI and PSII can not account for the fluorescence profile emitted by chloroplasts. This suggests that the procedure for isolating the photosystem fractions alters the energy transfer processes found in intact chloroplasts.

(1) Boardman, Thorne, and Anderson. 1966. PNAS. 56:586.
(2) Seibert and Alfano. 1974. Biophys. J. 14:269.
This work was supported in part by an NSF Grant.

TH-PM-L4 BICARBONATE EFFECT ON FLUORESCENCE TRANSIENTS IN TRIS-WASHED AND HEAT TREATED CHLOROPLASTS WITH VARIOUS ELECTRON DONORS. T. Wydrzynski* and Govindjee, Departments of Botany, Physiology and Biophysics, University of Illinois, Urbana, Illinois 61801.

In the absence of bicarbonate ions, the fast chlorophyll a fluorescence transient of broken spinach chloroplasts shows a rapid initial rise. Upon addition of saturating amounts of HCO_3^- (10 mM), the fluorescence rise shows the usual biphasic kinetics characteristic of normal chloroplasts (Stemler and Govindjee, Photochem. Photobiol. 19 (1974) 227-232). The fast transient measured as a function of HCO_3^- concentration is qualitatively similar to the concentration dependence of the transient for a block of electron flow on the reducing (Q) side of system II (e.g., DCMU) rather than for a block on the oxidizing (Z) side (e.g., NH_2OH or heat-treatment). In Tris-washed chloroplasts, the bicarbonate effect on the fast transient is still present, using either hydroquinine (250 µM), diphenyl carbazide (2 mM), hydroxylamine (25 mM) or manganese (1 mM) as an electron donor to system II. The effect is also present in heat treated chloroplasts using 25 mM NH_2OH as electron donor. These results suggest a site of action of bicarbonate after the site of electron donation by these artificial donors. This research was supported by a grant from National Science Foundation (GB 36751).

TH-PM-L5 THE EFFECTS OF CARBOXYL GROUP MODIFICATION UPON DIVALENT CATION BINDING AND FLUORESCENCE CHANGES IN TRITON X-100 SUB-CHLOROPLAST PARTICLES. L. J. Prochaska* and E. L. Gross, Department of Biochemistry, Ohio State University, Columbus, Ohio 43210.

Chemical modification of carboxyl groups on the cloroplast membrane with a water-soluble carbodiimide plus a nucleophile inhibited both Ca^{2+} ion binding and divalent cation-induced structural and fluorescence changes. Both control and carbodiimide treated chloroplasts were subjected to Triton X-100 fractionation (Chl/Triton X-100 = 40). Control particles bound 3.2 and 4.6 μMoles Ca^{2+}/MgChl for PS I (TSF I) and PS II (TSF II) particles respectively. Particles treated with 1-ethyl 3(3-dimethylaminopropyl) carbodiimide [EDC] plus glycine ethyl ester (a nucleophile) bound 2.5 and 2.1 μMoles Ca^{2+}/MgChl for PS I (TSF I) and PS II(TSF II) particles respectively. Thus the PS II fraction not only bound the most Ca^{2+} but showed the greatest inhibition by the carbodimide treatment indicating that the majority of the binding sites reside on the PS II(TSF II) particle. Both Ca^{2+} and Na^{+} caused a decrease in the salt-induced fluorescence of control particles with the largest change in the PS I(TSF I) fraction. Using ^{14}C-glycine ethyl ester, the EDC-mediated incorporation of radioactive label into the chloroplasts corresponded to the inhibition of Ca^{2+} binding. Upon chloroform:methenol extraction (2:1, v/v) 50% of the label was in the protein fraction.

TH-PM-L6 DEVELOPMENT OF EXCITATION ENERGY DISTRIBUTION REGULATION BETWEEN PHOTOSYSTEMS I AND II DURING THE FINAL STAGES OF CHLOROPLAST MEMBRANE DIFFERENTIATION. D. J. Davis*, P. A. Armond,* E. L. Gross and C. J. Arntzen, (Intr. by G. P. Brierley, Department of Biochemistry, Ohio State University Columbus, Ohio 43210 and Department of Botany, University of Illinois, Urbana, Illinois 61801.

Etiolated peas greened under intermittent light (cycles of 2 minutes light, 2 hrs dark) contain plastids with full photochemical activity but incompletely developed photosynthetic units. The final stages of membrane differentiation were monitored after transfer of these plants to continuous light. During the first 8 hours of constant illumination, the light-harvesting pigment protein (LHPP) complex appeared and showed rapid accumulation. During the next 40 hrs, the LHPP accumulation occurred at a constant but lesser rate. A similar biphasic increase was observed with respect to the following parameters: Mg^{++} regulation of room temperature PS II fluorescence intensity; Mg^{++} effects on low temperature fluorescence emission spectra; low affinity (K_m= 0.05 mM) binding of divalent cations to the membranes; and appearance of grana stacks. We suggest that the insertion of a specific pigment-protein complex into the membrane is the factor regulating the control of excitation energy distribution between PS I and PS II in chloroplast lamellae.

TH-PM-L7 REGULATION OF EXCITATION ENERGY DISTRIBUTION BETWEEN PHOTOSYSTEMS I AND II IN DEVELOPING CHLOROPLASTS. P.A. Armond* and C.J. Arntzen, Department of Botany, University of Illinois, Urbana, Illinois 61801.

Etiolated pea seedlings were greened for 2 days under intermittent light (cycles of 2 min light, 2 hrs dark). Plastids isolated from these plants exhibited high rates of photosystem I and II electron transport, photophosphorylation, and "proton-pump" activities. Light saturation curves indicated smaller photosynthetic unit sizes in these plastids. Electron microscopic examination of the samples showed plastids with no grana stacks. The light harvesting pigment protein complex (SDS solubilized membranes; polyacrylamide disc gel electrophoresis: Thornber and Highkin (1974) Eur. J. Biochem. 41:109-116) was also absent in these plastids. Etiolated pea leaves which were greened under intermittent light and then under continuous light for 24 hours had grana-containing plastids which had normal size photosynthetic units and which contained the light harvesting pigment protein complex. Addition of Mg^{++} to the "continuous light" chloroplasts increased room-temperature fluorescence yield, decreased PSI fluorescence at liquid nitrogen temperature, and decreased the rate of PSI reactions measured at limiting light intensity. None of these effects were observed with the "intermittent light" chloroplasts. The appearance of the light harvesting pigment protein complex, of grana, and of Mg^{++} regulation of excitation energy distribution between photosystems I and II seem to be causally related.

TH-PM-L8 SILICOMOLYBDATE AND SILICOTUNGSTATE MEDIATED DCMU-INSENSITIVE PHOTOSYSTEM II REACTION: ELECTRON FLOW, CHLOROPHYLL *a* FLUORESCENCE AND DELAYED LIGHT EMISSION CHANGES. B. Zilinskas and Govindjee, Departments of Botany and Physiology and Biophysics, University of Illinois, Urbana, Illinois 61801.

Girault and Galmiche (Biochim. Biophys. Acta, 333, 314, 1974) and Giaquinta *et al.* (Biochem. Biophys. Res. Comm. 59, 985, 1974) have shown a DCMU-insensitive oxygen evolution from photosystem II in the presence of silicotungstate (SiTu) and ferricyanide, and silicomolybdate (SiMo) and ferricyanide, respectively. We investigated the possible role of SiMo and SiTu as acceptors of electrons in chloroplasts from Q, the primary electron acceptor of photosystem II. Data show that both these compounds accept electrons from Q in a DCMU-insensitive electron transport; however, the DCMU insensitivity is only short-lived, so initial rates must be used exclusively. High concentrations ($\geq$ 50 μM) of these silico-compounds act as quenchers of chlorophyll *a* fluorescence at the Fo level, but lower concentrations ($\leq$ 25 μM), which also mediate oxygen evolution, affect only the variable (F_∞ - Fo) component of fluorescence in a manner suggestive of their electron accepting abilities. Measurements of the 100 msec component of delayed light emission (DLE) confirm the conclusions made from the fluorescence data. Also, they show the role of Q in DLE as hydroxylamine data have shown the role of Z, the electron donor of photosystem II. Silico-compounds appear to act as electron acceptors and not as simple membrane modifiers allowing other acceptors to support a DCMU-insensitive electron transport.

TH-PM-L9 DISSOCIATION OF THE BACTERIOCHLOROPHYLL REACTION-CENTER COMPLEX FROM GREEN BACTERIA. John M. Olson, Thomas H. Giddings, Jr.* and Elizabeth K. Shaw*, Biology Department, Brookhaven National Laboratory, Upton, New York 11973.

Bacteriochlorophyll reaction-center complexes from *Chlorobium thiosulfatophilum*, strain 6230 (Tassajara), were incubated for 30 min in 2 M guanidine-HCl in 10 mM Na phosphate (pH 7.4) and 10 mM ascorbate and then chromatographed on Sephadex G-100 or -200. Each fraction was characterized by absorption spectrum and circular dichroism spectrum for the Q_y-band of bacteriochlorophyll. At least two components of the complex were partially separated as a heavier fraction (A) with a relatively high shoulder at 835 nm in the absorption spectrum and a lighter fraction (B) with no sign of a shoulder at 835 nm. The circular dichroism spectra of fractions A and B were strikingly different from each other. Light-induced cytochrome oxidation was demonstrated in both components. In fraction A the light-on reaction was approximately 6-10 times faster than in fraction B. Also the steady state level of oxidation in the light in fraction A was about twice the level in fraction B. Fraction A appears to be enriched in reaction center, whereas fraction B appears to be enriched in bacteriochlorophyll-protein. Research carried out at Brookhaven National Laboratory under the auspices of the U. S. Atomic Energy Commission.

TH-PM-L10 A PROPOSAL FOR THE PRIMARY PHOTOCHEMICAL EVENTS OF BACTERIAL PHOTOSYNTHESIS. P. A. Loach, Department of Biochemistry and Molecular Biology, Northwestern University, Evanston, Illinois 60201.

Substantial evidence has accumulated which is consistent with a role for ubiquinone as the primary electron acceptor in R. rubrum and R. spheroides. As a result of light absorption, the first stable products whose oxidation states have changed would be $[BChl]_n^{+\cdot}$ and $UQ^{-\cdot}$ where n = 2 to 4. In the following postulate, the multiple redox equilibria of quinones is utilized to allow one quinone molecule to interact with two bacteriochlorophyll donor units. Under saturating light conditions in chromatophores,

$$[BChl]_4 \square UQ \square [BChl]_4 \xrightarrow{+\ 1h\nu} [BChl]_4 \square UQ^{-\cdot} \square [BChl]_{2-4}^{+\cdot} \longrightarrow \left[\begin{array}{l}\text{rapid protein con-}\\ \text{formational change}\\ \text{and/or protonation}\\ \text{of } UQ^{-\cdot}\end{array}\right]$$

$$\longrightarrow [BChl]_4 \square UQH^{\cdot} \triangle [BChl]_{2-4}^{+\cdot} \xrightarrow{+\ 1h\nu} [BChl]_{2-4}^{+\cdot} \square UQH^{-} \triangle [BChl]_{2-4}^{+\cdot}$$

$$\longrightarrow \left[\begin{array}{l}\text{rapid protein}\\ \text{conformational}\\ \text{change and/or pro-}\\ \text{tonation of } UQH^{-}\end{array}\right] \longrightarrow [BChl]_{2-4}^{+\cdot} \mathbin{/\!/} UQH_2 \triangle [BChl]_{2-4}^{+\cdot} \longrightarrow \left[\begin{array}{l}\text{2ndary electron}\\ \text{transport and/or}\\ \text{displacement of}\\ UQH_2 \text{ with UQ}\end{array}\right]$$

The following observations are explained with the above scheme: a) No requirement for iron. b) No e. s. r. due to electron acceptor under saturating light conditions. c) Procedures that disrupt the membrane structure (e.g., AUT-e) remove one donor unit and allow observation of $UQ^{-\cdot}$ or $UQH\cdot$. d) Only half of $[BChl]_{2-4}^{+\cdot}$ is photo-reversibly formed at low temperature. e) Two cytochromes can be photoxidized on successive laser pulses. f) ϕ for cytochrome oxidation = 1.0. g) Extension of the scheme to two photosystems, or to explaining the two equivalents of Q in PS II of O_2 evolving organisms has obvious applications.

TH-PM-L11 PICOSECOND ABSORPTION KINETICS OF RPS SPHEROIDES. K. J. Kaufmann, T. L. Netzel, P. L. Dutton, J. S. Leigh and P. M. Rentzepis. (Intr. by J. Eisinger), Bell Laboratories, Murray Hill, New Jersey 07974, and Johnson Research Foundation University of Pennsylvania, Philadelphia, Pa. 19174.

Time-resolved absorption spectroscopy has been performed on preparation from photosynthetically grown Rps spheroides in combination with redox potentiometry. Examination of the 500-650 nm, 800-900 nm and 1250 nm spectral range reveal new transients including lifetimes between 5-100 psec. Implications of these results with respect to the current attitudes of P870 as a functional dimer will be critically discussed.

TH-PM-L12 MOSSBAUER STUDY OF REACTION CENTERS FROM R. SPHEROIDES P.G. Debrunner and C.E. Schulz* Physics Department, University of Illinois, Urbana, Ill. and G. Feher and M.Y. Okamura, Physics Department, University of California, San Diego, Calif. 92037

We have measured Mossbauer spectra of ^{57}Fe-enriched preparations of purified reaction centers from the photosynthetic bacterium R. spheroides R-26. Non-reduced samples (N) and dithionite-reduced samples (R) were studied. (R) showed the characteristically broad low-temperature EPR signal (Feher (1971) Photochem. Photobiol. 14 373; Dutton, Lee and Reed (1973) BBA 292 654). The Mossbauer spectra of both (N) and (R) consist of quadrupole doublets with a temperature dependent splitting $\Delta E_Q(T)$ given in the Table below and, for $T < 100°K$, an isomer shift relative to iron metal of 1.125 ± 0.010 and 1.10 ± 0.01 mm/sec for (N) and (R) resp. (R) shows line broadening at low temperature indicative of magnetic hyperfine interaction. In an applied field H_0 the lines broaden in a way characteristic of paramagnetic samples, the internal field H_i being somewhat larger for (R). Even at 25kG and 4.2°K little structure is seen in the spectra. On the basis of these measurements we conclude that the iron in both samples is in a high-spin ferrous state (Fe^{2+}, $S = 2$). For the reduced sample the results are consistent with the production of a free radical which weakly couples with the iron and causes a slight decrease in its isomer shift and quadrupole splitting and presumably is also responsible for the larger internal field H_i.

T (°K)		4.2	20	40	60	80	100	120	150	190
$\Delta E_Q(T)$ (mm/sec)	(N)	2.19	2.18	2.19	2.19	2.16	2.13	2.07	2.00	1.83
	(R)		2.10	2.09	2.08	2.05	1.98	1.94	1.86	1.75

Supported by Grants from NSF, BMS 74-21413, and NIH, GM-13191 and GM-16406.

TH-PM-M1 THE EFFECT OF AMILORIDE AND SOME OF ITS ANALOGUES ON CATION TRANSPORT IN BLACK LIPID MEMBRANES AND ISOLATED FROG SKIN. D.J. Benos*, S.A. Simon*, and L.J. Mandel, Department of Physiology and Pharmacology, Duke University Medical Center, Durham, North Carolina 27710.

The diuretic drug amiloride is a potent inhibitor of Na^+-transport in a wide variety of cellular and epithelial systems. We have performed experiments on planar phospholipid bilayer membranes and on isolated frog skin in order to: (1) test the effect of amiloride on a carrier-mediated ion transport system in bilayers; (2) determine whether the charged or uncharged form of amiloride is the effective Na^+-transport inhibitor in frog skin; and (3) study the ability of a wide variety of amiloride analogues to inhibit Na^+-transport in frog skin. In egg lecithin-decane bilayers separating symmetrical solutions of 10^{-1}M KCl and 10^{-8}M nonactin (either at pH 5.6 or 10.5), 10^{-4}M amiloride decreases the nonactin-induced K^+-conductance; the magnitude of this decrease is consistent with about a +25 mV increase in the surface potential of the bilayer. The magnitude of the amiloride inhibition of net Na^+-transport in isolated frog skin is constant from pH 6 to 9. Above pH 9 the percent inhibition is drastically reduced, amiloride becoming completely ineffective at pH 11. These results are consistent with the idea that in frog skin the active form of amiloride is the charged species. Amiloride appears to be very specific in its inhibitory interaction with the Na^+-transport mechanism, since slight modifications of the molecule result in significant changes in effectiveness. Our results suggest that amiloride binds to and alters the charge on membrane surfaces, but this action cannot explain its highly specific effects in biological systems. (Supported by NIH Grants HL-12157 and AM-16024. DJB was supported by NIH Training Grant No. 5 T01 GM-00929.)

TH-PM-M2 SECRETION AND CELL pH AS MEASURED BY DMO DISTRIBUTION IN GASTRIC MUCOSA. L.Villegas, E.González*, T.Kirchhausen* and L.Sananes. Centro de Biofísica y Bioquímica, Instituto Venezolano de Investigaciones Científicas, IVIC, Caracas, Venezuela.

Simultaneous measurements of inulin-H3 and DMO-C14 distribution were used to estimate the cell pH (pHc) in frog gastric mucosa. The DMO cell activity was calculated by subtracting from the tissue C-14 activity that of the inulin space and dividing the difference by the cell water. The solutions used were buffered with HCO_3^- bubbled with 95-5 O_2-CO_2. The mean ratios DMO_c/DMO_o for groups of 20 mucosae each, incubated in Cl^- solutions with pH_o of 5.90, 6.90 and 7.96 were: 3.6±0.2, 3.4±0.3 and 1.0±0.1 for the non-stimulated mucosae and 4.8±0.4, 6.1±0.4 and 2.4±0.1 for the mucosae stimulated with 10^{-4}M histamine. From the pK_a (6.27) and the ratios obtained for each mucosa, mean pH_c of 6.86±0.04, 7.47±0.04 and 7.95±0.03 were calculated for the three groups of non-stimulated mucosae and 7.00±0.04, 7.74±0.03 and 8.23±0.03 were calculated for the three groups of histamine stimulated mucosae. In the three points the mean pH_c is higher ($P<0.02$) in the stimulated than in the non-stimulated mucosae. Correlation coefficients of 0.95 and 0.96 between the pH_c and the pH_o were obtained. The regression coefficients ($\Delta pH_c/\Delta pH_o$) obtained by fitting the results to straight lines were: 0.53±0.02 for the non-stimulated mucosae and 0.62±0.02 for the histamine stimulated mucosae. According to these results the pH_c increases during histamine stimulated secretion. This increment in pH_c can be explained by the opening of the vesicotubules, filled with low pH medium, to the secretory surface. The apparent change in the slope $\Delta pH_c/\Delta pH_o$ must be related to the change in area of the cell membrane and/or to permeability change during histamine stimulation.

TH-PM-M3 THE Na POOL AND Na FLUXES ACROSS INNER AND OUTER BARRIERS OF FROG SKIN EPITHELIUM. O.A.Candia and P. Reinach‡Department of Ophthalmology, Mount Sinai School of Medicine of CUNY,New York, N.Y. 10029.

Epithelium(15 cm^2) from bullfrog skin was mounted extended in a thin plastic frame and incubated for 2 hrs in 22-Na Ringer. Following this, the epithelium was transferred to a 20 ml-volume washout chamber with a solution continuously circulating in a closed system including a γ detector. 22-Na in the washout solution was measured until equilibrium. This washout curve reveals 2 components. The fast one, with a $T_{\frac{1}{2}}$ of less than 1 min,represents an extracellular compartment. The slower component has a $T_{\frac{1}{2}}$ of 5.9 min under control conditions and a $T_{\frac{1}{2}}$ of 12 min in ouabain treated epithelium. This suggests that the slower component represents Na from a cellular pool. The size of this pool was 0.35 $\mu eq/cm^2$ for the control and 0.80 $\mu eq/cm^2$ for the ouabain treated epithelium. In other experiments, the 22-Na loaded epithelium was mounted in a 7 cm^2 Ussing-type chamber and the loss of 22-Na to the outside and inside solutions was measured simultaneously under short-circuit condition. It was found that no 22-Na is lost to the outside solution in control epithelia and very little in the ouabain treated. The rate of 22-Na loss to the inside solution was equal to that determined in the washout chamber with both surfaces exposed to the same solution. Our results show that: 1. The backleak across the outside barrier is negligible; 2. The Na uptake by the outside barrier is equal to the transepithelial transport (0.7 $\mu eq/hr.cm^2$); 3. The rate of transfer of Na from the epithelial cells to the inside solution is 2.8 $\mu eq/hr.cm^2$; 4. Ouabain inhibits both the Na uptake by the outside barrier and the pump component at the inside barrier but increases both the diffusion rate across the inside barrier and the Na pool.

Supported by Am.Heart Assn.Grant 72-846 and NIH Fellowship to P. Reinach

TH-PM-M4 ION SELECTIVITY OF THE PARACELLULAR PATHWAY IN NECTURUS PROXIMAL TUBULE. Mary F. Asterita* and Emile L. Boulpaep, Department of Physiology Yale University School of Medicine, New Haven, Conn. 06510.

Transepithelial conductance both in mammalian and amphibian proximal tubule is dominated by a paracellular shunt. The present experiments investigate whether overall ion selectivity of the proximal tubular epithelium of Necturus kidney resides entirely in the paracellular path. Changes in peritubular cell membrane (ΔV_1), luminal cell membrane (ΔV_2), or transepithelial potential (ΔV_3) were monitored during single sided salt dilutions in the peritubular capillaries (p), or in the lumen only (ℓ), or bilaterally ($p\ell$). NaCl salt dilutions p or ℓ lead to ΔV_3's where the diluted compartment becomes more negative. Calculated transference numbers are T_{Cl}=0.71, and T_{Na} = 0.29. Salt gradients of equal magnitude but of reversed direction yield identical ΔV_3's of opposite sign. At equal salt concentration ratio ΔV_3 is independent of absolute concentrations used. Observed ΔV_3 is not due to interference with active transport or with the electromotive forces at the individual cell membranes. A comparison of ΔV_1 and ΔV_2 during p, ℓ, and $p\ell$, substitution proves the latter point. Actual changes in electromotive forces induced across the peritubular membrane (ΔE_1), luminal membrane (ΔE_2), and paracellular path (ΔE_3) were estimated from simultaneous equations for ΔV_1 and ΔV_2, during p, ℓ, or $p\ell$, and from the luminal to peritubular cell membrane resistance ratio determined experimentally. Cellular and paracellular resistances were assumed to remain constant during salt dilution. The results indicate that ΔV_3 is a close estimate of ΔE_3. Hence, the observed transepithelial potential changes in a "leaky" epithelium provide an accurate estimate of paracellular ionic selectivity.

Supported by USPHS Research Grant 5-R01-AM-13844.

TH-PM-M5 MODERATORS OF ACTIVE ANION TRANSPORT IN TURTLE BLADDERS., W.A. Brodsky, J. Parkes* and T.P. Schilb., Mount Sinai Sch. Med./CUNY, and Louisiana State Univ. Med. Ctr., New Orleans.

When isolated turtle bladders are bathed by Na-free (choline) Ringer solutions, the short-circuiting current (I_{SC}) equals the sum of the net m-to-s flux of ($Cl^- + HCO_3$), of Cl alone, or of HCO_3 alone - depending on which anion (s) is present in the mucosal fluid. Serosally applied acetazolamide (a carbonic anhydrase inhibitor) inhibits the transport of HCO_3 and/or Cl - which prompted a look at the transport effects of carbonic anhydrase (CAH) "stimulators" (e.g. histidine, histamine, imidazole). These CAH stimulators increased the anion-related I_{SC}, but their action was elicited only from the mucosal fluid side - which implies that acetazolamide penetrates the basal-lateral membrane and histamine etc penetrate the apical membrane, while CAH is located in the cytoplasm. However, histamine is a known stimulator of hepatic adenyl cyclase - which implies that mucosally applied CAH "stimulators" increase the activity of adenyl cyclase in the apical membrane. It is known that histamine increases hepatic adenyl cyclase (Sutherland, 1962) which suggests that the CAH stimulators were really stimulating adenyl cyclase, and that an adenyl cyclase system in the apical membrane regulates anion transport in the turtle bladder. In keeping with this suggestion, nor-epinephrine or theophylline added to the mucosal (and not to the serosal fluid) was followed by a two-to-threefold increase in the HCO_3-related and Cl-related I_{SC} - which means that these agents increase the active transport of Cl and HCO_3. It is proposed that nor-epinephrine is the first (hormonal) messenger for stimulating an intra-apical membrane cyclase on its luminal surface. The resulting release of cAMP then acts to increase the rate of anion transport at an unspecified membrane site.

TH-PM-M6 ESTIMATION OF WIDTHS OF SLITS BETWEEN CAPILLARY ENDOTHELIAL CELLS BY TRACER AND OSMOTIC METHODS. J.B. Bassingthwaighte, E.F. Grabowski*, E. Bouskela*, and T.J. Knopp*, and T. Yipintsoi*, Dept. of Physiology and Biophysics, Mayo Grad. Sch. Med., Rochester, Minn. 55901, and Montefiore Hospital, Bronx, N.Y. 10467.

Using multiple tracer indicator dilution curves recorded from the outflow from isolated Langendorff-perfused dog and rabbit hearts, estimates of the permeability-surface area products PS were obtained for a variety of small hydrophilic solutes of differing molecular size. By comparing the ratios of estimated PS's for pairs of solutes with the ratios of free diffusion coefficients, the degree of restriction to transcapillary membrane passage was estimated. The apparent PS for sucrose, for example, was about 20% less than that predicted from that for potassium, suggesting that the slit widths were more than 10 times the radius of sucrose (5.3 Angstroms). In osmotic transient experiments, we made observations on changes of weight of rabbit hearts after negative or positive step changes in perfusate osmolarity using albumin, NaCl, sucrose, raffinose, and inulin (and after step changes in perfusion pressure), and analysed the families of curves using a model for the movements and concentrations of water, protein, electrolytes and test solute species in an organ composed of capillaries, interstitial space, and cells. These data gave sets of estimates of PS and of reflection coefficients which implied slit widths of about 100 Å. In experiments using ^{14}C-sucrose injection during osmotic weight transients, no effect of the direction of the water flux on PS for sucrose was seen, suggesting that solvent drag is small. (Supported by NIH grant HL9719.)

TH-PM-M7 DIFFUSION RESISTANCE OF ENDOTHELIUM AND STROMA OF BULLFROG CORNEA DETERMINED BY POTENTIAL RESPONSE TO K^+. C. N. Graves,* S. S. Sanders, R. L. Shoemaker and W. S. Rehm. Dept. of Physiol. and Biophys., Univ. of Ala. in Birmingham, The Medical Center, Birmingham, Ala. 35294

Corneas of bullfrog (Rana catesbeiana) were mounted between lucite chambers. A four electrode system was used and the potential difference (PD) and the electrical resistance were measured. In intact corneas the PD averaged 25 mv (aqueous side positive) and the electrical resistance 1.5 kilo ohm cm^2. Perfusion of the aqueous side with high K^+ solutions resulted in a marked decrease in PD and a drop in the electrical resistance. Scraping the epithelium (leaving the stroma plus endothelium) resulted in a drop of the PD to about zero and a decrease in electrical resistance to about 0.1 kilo ohm cm^2 and a very small PD response to a marked elevation of the K^+ concentration on the aqueous side. On the basis of the above it is obvious that the large ΔPD in intact corneas due to elevation of the K^+ concentration, must be due to K^+ diffusing from the aqueous side across the endothelium and stroma and reaching the epithelium. The duration of the PD response is therefore a measure of the resistance to diffusion of the stroma plus endothelium. A quantitative analysis based on the finding that the PD vs log $[K^+]$ is linear (from 5 to 80 mM) and on a solution of Fick's equation for a homogeneous diffusion barrier shows that under in vitro conditions the resistance of the endothelium plus stroma to the diffusion of ions is very low. (NIH and NSF support.)

TH-PM-M8 EFFECTS OF AMPHOTERICIN B ON THE ELECTRICAL PARAMETERS AND THE SODIUM PERMEABILITY OF THE AMPHIBIAN LENS. P.J.Bentley* and O.A.Candia, Intr. by I.L.Schwartz. Departments of Ophthalmology and Pharmacology, Mount Sinai School of Medicine of CUNY. New York, N.Y. 10029.

The polyene antibiotic amphotericin B decreases the PD and short-circuit current (scc) across the amphibian lens isolated in an Ussing-type chamber. It was only effective when placed in the solution at the anterior side. The effect was reversible when the drug was removed from the bathing solution. It was found (with a third electrode inserted in the lens fibers) that amphotericin B caused a large decline in the PD across the anterior surface of the lens and this was accompanied by a smaller reduction in the PD across the posterior side. The electrical effects seem to be due to a direct decrease of the electrical resistance of the anterior face that acts as a shunt to the ionic pump, associated with an indirect and smaller increase of the resistance of the posterior face. The effects depended on the presence of sodium in the Ringer solution bathing the anterior surface of the lens while removal of it at the posterior surface or chloride from either side had no effect. The translenticular fluxes of Na were increased in both directions by a similar amount so that the net flux changes little. Amphotericin B produced a considerable increase in the rate of accumulation of sodium and loss of potassium by the lens. The oxygen consumption of the lens was unchanged by amphotericin B which contrasts to the drug's effects on other epithelial membranes, as well as that of ouabain which has similar effects on the PD, SCC and ionic content of the lens. Amphotericin B appears to act on the lens epithelium by selectively increasing its passive sodium permeability.

Supported by NIH grant EY 01278 and American Heart Association grant 72-846.

TH-PM-M9 CAPACITIVE AND INDUCTIVE REACTANCES ACROSS RABBIT CORNEAL ENDOTHELIUM. J. J. Lim and J. Fischbarg, Depts. of Ophthalmology and Physiology, College of Physicians and Surgeons, Columbia University, New York.

A.C. and D.C. electrical characteristics of rabbit corneal endothelium have been studied under varying experimental conditions. In addition to the capacitive reactance reported earlier, an inductive reactance was also found at the lower frequency range. A.C. measurements were performed between 0.5 Hz and 100 KHz; the current across the preparation (for both the A.C. and D.C. cases) was 10μAmps. The transendothelial potential difference was measured during the intervals between A.C. determinations. When plotted in the R-X plane, the capacitive circular arc "above" the real axis was continued at the low frequency end by a curve of a smaller radius "below" the real axis, which ended at a point (D.C. resistance value) between the origin and the frequency of zero reactance (usually in the range 10-100 Hz). In some experiments, the "capacitive" arc consistently deviated from its usual circular shape, and its radius of curvature progressively decreased with increasing frequency. Both findings were taken to suggest the presence of an element with inductive behavior in the preparation. The shape and size of these curves were affected in a consistent fashion by such experimental manipulations as: a)presence of $5x10^{-5}$M ouabain; b)absence of ambient HCO_3, and c)absence of nutrients (glucose, adenosine). Some simple equivalent electrical circuits can be made to exhibit a behavior close to that of the experimental data by adjusting their parameters (resistors, capacitor, inductor). Possible relationships between the equivalent electrical parameters and some morphological characteristics of the endothelial layer will be presented.

TH-PM-M10 AN ELECTRICAL EQUIVALENT CIRCUIT OF ISOLATED FROG SKIN AS VIEWED FROM ITS CURRENT-VOLTAGE RELATIONSHIP. S.I. Helman, Dept. of Physiology & Biophysics, University of Illinois, Urbana, Illinois 61801

When isolated frog skins are studied in the absence of edge damage, their steady-state current-voltage (I-V) relationships show electrical rectification at voltages previously defined E_1 and E_2. These voltages are thought to give direct estimates of the emf's of the ion pumps of the skin. The I-V relationship can be modeled with an equivalent circuit that consists of three distinct and separate parallel paths. Ion flows in the active paths containing the emf's E_1 and E_2 are limited by the resistances of the diodes D_1 and D_2, where subscript 'f' indicates flow from pond to blood side and subscript 'b' indicates flow in the reverse direction. The third path is considered to be an entirely passive shunt resistance, R_s. Together, these elements of the equivalent circuit account for the unique pattern of electrical rectification. From knowledge of the parameters of the I-V relationship, the values of the resistances of the equivalent circuit can be calculated directly. Thus it is possible to obtain estimates simultaneously not only of the emf's of the ion pumps, but also estimates of their series resistances in this epithelium which consists of multiple parallel ion transport pathways. (Supported by USPHS Grant AM-16663.)

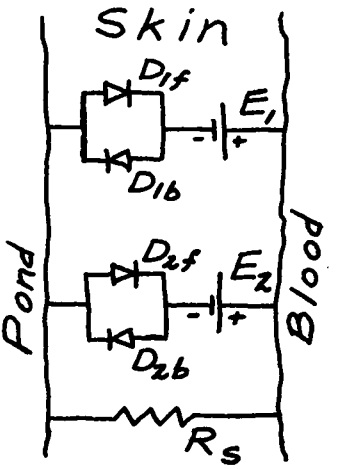

TH-PM-M11 LOCATION OF A TRANSPORT-RELATED CONDUCTANCE PATHWAY IN RABBIT URINARY BLADDER, A TIGHT EPITHELIUM. S.A. Lewis*, D.C. Eaton[1] and J.M. Diamond, Dept. of Physiology, UCLA Medical School, Los Angeles, California 90024. 1. Dept. of Physiology and Biophysics, Univ. of Texas Medical Branch, Galveston, Texas 77550.

In previous experiments on rabbit urinary bladder we showed that net Na^+ transport from lumen to blood equals the short-circuit current ($I_{s.c.}$), and that transport is stimulated by aldosterone and inhibited by amiloride. A special mounting technique was used to eliminate virtually all edge-damage conductance, and tissue capacitance was used to normalize for epithelial surface area (1 μfarad ∿ 1 cm^2 of tissue). $I_{s.c.}$ and transepithelial resistance (R) proved to be inversely correlated, such that at zero $I_{s.c.}$ R reaches a high of 62,000 Ω-μfarad, while R declines to 7500 Ω-μfarad at $I_{s.c.}$ = 20μamp/μfarad. The present study focuses on the location of this transport-related conductance change. By microelectrode methods, we found that with increasing $I_{s.c.}$ the conductance of the luminal membrane increases linearly but the conductance of the baso-lateral membrane shows little or no change. Luminal membrane conductance decreases with amiloride inhibition of transport but increases with aldosterone stimulation of transport. We conclude that the rate-limiting step for Na^+ transport from bladder lumen to plasma is a Na^+ conductance pathway located in the luminal membrane, and that one action of aldosterone is to increase the conductance of the luminal membrane.

TH-PM-M12 PARACELLULAR SHUNT RESISTANCE AND TRANSMURAL ELECTRICAL PROPERTIES OF SMALL INTESTINE. W. McD. Armstrong, S.J. Cohen* and C.J. Myers*. Department of Physiology, Indiana University School of Medicine, Indianapolis, Indiana 46202

Equivalent electrical circuits analogous to that shown were successfully invoked to explain effects of actively transported sugars and amino acids on measured P.D. (E_{Tr}) across isolated bullfrog and rabbit small intestine. V and R are e,m,f's and resistances. m, s and j refer to the mucosal and serosal epithelial cell membranes and to a low resistance paracellular shunt. V_j is assumed to arise from transcellular solute transfer from lumen to lateral intercellular spaces. Analysis of this circuit for E_{Tr} and I_{sc} (short circuit current) gives

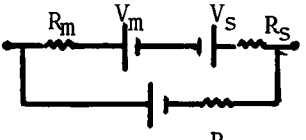

$$E_{Tr} = \left[(V_s - V_m)\, R_j - V_j (R_m + R_s)\right] / \left[R_m + R_s + R_j\right] \text{ and}$$

$$I_{sc} = \left[(V_s - V_m)/(R_m + R_s)\right] - V_j/R_j.$$

Thus, if $R_j \ll (R_m + R_s)$ and $0 \ll V_j < (V_s - V_m)$ E_{Tr} (serosal positive) should vary directly with R_j. If $V_j > 0$, I_{sc} should also vary directly with R_j. Changes in E_{Tr} and I_{sc} consistent with these predictions were found when sheets of isolated bullfrog small intestine were mounted between symmetrical sodium sulfate media of varying osmolality but constant ionic composition. It is concluded that (1) under these conditions V_j is not negligible compared to $(V_s - V_m)$, (2) responses of E_{Tr} and I_{sc} to changes in R_j alone are essentially coupled, (3) I_{sc} in small intestine, though it may correspond to net m→s Na^+ transport, does not necessarily reflect the intrinsic rate of m→s Na^+ pumping by this tissue. (Supported by USPHS grants AM 12715, HL 06308).

TH-PM-M13 PROGRAMMABLE CONTROL SYSTEM FOR INVESTIGATING FACTORS MODULATING REFRACTORY PERIODS OF CELL MEMBRANES. Christopher Druzgalski* and Philip B. Hollander, Ohio State Univ., Col. Med., Dept. Pharmacol., Columbus, Ohio 43210.

An investigation of the refractory period using test stimuli would aid in defining parameters of cell membranes as influenced by drugs. Present analysis relies on increasing stimulus frequency or extra pulses at specific intervals. We have developed a digital control system to deliver single or sequential stimuli. This system is a stimulating unit and/or a triggering unit producing delayed output pulses in the range of 0-999 msec adjustable in 1 msec increments, facilitating programming of repetitive activities for estimation of refractoriness. The system, designed around monolithic circuits and thumbwheel adjustments, has the following characteristics: triggering pulse amplitude of 5-15 V; pulse duration from 0.5 msec; selection of independent or common output adjustment; visual observation of pulses; and the output can drive TTL or interface with other stimulators. Preliminary experiments using *in vitro* mammalian ventricle muscles driven at 60/min, maintained in 30°C Krebs-Henseleit medium with a pH = 7.4 when gassed with 95% O_2 - 5% CO_2 have produced a mean functional refractory period of 360 msec when tissues were excited via intracellular microelectrodes with threshold stimuli of about 0.7 μA which is less than 10^{-11} equivalent Wt/sec or 10^{-13} moles/cm^2. This system appears capable of improving recognition and aiding interpretation of cell membrane phenomena related to excitation and conduction. (Supported in part by NIH grants HE-09567 and HL-11,929 and a grant from the American Heart Association, Central Ohio Chapter.)

TH-PM-N1 THE LINKAGE BETWEEN OXYGENATION AND SUBUNIT DISSOCIATION IN HUMAN HEMOGLOBIN. G.K. Ackers and H.R. Halvorson, Department of Biochemistry, University of Virginia, Charlottesville, Virginia 22901.

The use of subunit dissociation as a means of probing intersubunit contact energy changes which accompany cooperative ligand binding has been studied for the case of human hemoglobin. An analysis is presented delineating the information that can be obtained from the linkage relationships between ligand binding and subunit dissociation of hemoglobin tetramers into dimers. The analysis defines (a) The variation of the saturation function, $\bar{Y}$ with total protein concentration (b) The variation of the subunit dissociation constant $^{X}K_2$ with ligand concentration, (X) (c) The correlations between changes in dimer-dimer contact energy and the sequential ligand binding steps. It is shown that an unambiguous resolution of the cooperative energy expended within the contact region between ($\alpha\beta$) dimer pairs can be achieved corresponding to three stages of ligation: The first ligand binding step, the second two binding steps, and the fourth binding step. It is not possible to separate the relevant energy terms pertaining to the second and third steps without additional information. The information required is the equilibrium distribution of ligand on doubly-liganded tetramers, with respect to the ($\alpha^1\beta^1$) and ($\alpha^2\beta^2$) pairs. Sensitivity of the linkage functions has been explored by numerical simulation. It is shown that subunit dissociation may appreciably affect oxygenation curves under usual conditions of measurement and that relying solely on either $^{X}K_2$ or $\bar{Y}$ may lead to incorrect pictures of the energetics, whereas the combination defines the system more exactly.

Supported by USPHS Grant GM-14493.

TH-PM-N2 IN VITRO ASSEMBLY OF SALMONELLA FLAGELLAR FILAMENTS FROM NORMAL, CURLY, AND STRAIGHT MUTANTS. Bernard R. Gerber, Department of Biology, University of Pennsylvania, Philadelphia, Pennsylvania 19174.

To explain the formation of a long period helix in the tubular protein filaments of bacterial flagella, Klug (Symp. Int. Soc. Cell Biol. (1967), 6, 1-18) proposed that the constituent protomers might assume two or more of a limited number of conformations which he referred to as "quasi-equivalent states." Thus, protomers on an inner surface would have to be smaller than those on an outer surface of the helical tubule. The existence and magnitude of an energy difference between such hypothetical conformational states was evaluated from the temperature dependence of the kinetics for polymerization and depolymerization of flagellar filament protein as measured in Ostwald-type viscometers. Filaments from flagellar shape mutants N, C, and S with helical pitch of approximately 2.5, 1.2 and 0 μm, respectively, were used. Analysis of kinetic data obtained earlier on N and C (Gerber, Asakura and Oosawa, J. Mol. Biol. (1973) 74, 467-487) and those from S filament protein yield enthalpy values (ΔH) in kcal/mole for the reaction $M \rightleftharpoons P$ of $\Delta H_N = 38$, $\Delta H_C = 43$, and $\Delta H_S = 50$. The assembly of protomers in the identical state should result only in straight tubules. If N, C and S monomers are in the same energy state, the difference enthalpies ($\Delta H_N - \Delta H_S$) = -12 kcal/mole and ($\Delta H_C - \Delta H_S$) = -7 kcal/mole might represent destabilization energies introduced by packing protomers into N and C helical filaments. This destabilization would permit protomers to assume different packing rearrangements which would serve to propagate waves along a flagellum and so move the bacterium.

Support by National Science Foundation Grant No. GB29367 is gratefully acknowledged.

TH-PM-N3 ENTROPY-DRIVEN POLYMERIZATION OF TOBACCO MOSAIC VIRUS PROTEIN. Max A. Lauffer, Department of Biophysics and Microbiology, University of Pittsburgh, Pittsburgh, Pa. 15260.

The coat protein, TMVP, of tobacco mosaic virus polymerizes above pH 7 to form double discs and at somewhat lower pH values to form helical rods. In 1958, it was observed in our laboratory that this polymerization is endothermic and, therefore, entropy-driven. Subsequent investigations carried out by the author and his colleagues have established the following facts. Polymerization can be carried out reversibly. The positive enthalpy and entropy of polymerization have been evaluated from the variation of the equilibrium constant with temperature; the positive enthalpy has been verified calorimetrically. Polymerization is enhanced by an increase in ionic strength and by a decrease in pH. It is accompanied by the binding of hydrogen ions; at pH values above about 4.7 this is a thermodynamic liability. Reducing the pH lowers the liability and thus promotes polymerization. Other ions seem not to be bound or released during polymerization. Polymerization is accompanied by an increase in volume, demonstrated dilatometrically. The increase in volume and the increase in entropy needed to drive the polymerization have been shown experimentally to come from the release of "bound" water molecules, approximately 26 per protein subunit. Chemicals which break the structure of water inhibit polymerization; those which increase structure favor it. The polymerization of TMVP resembles in many respects entropy-driven polymerization of tubulin, sickle cell hemoglobin, collagen, actin, myosin, flagellin and other biologically important molecules. Because of this, it is a reasonable inference that the source of the entropy increase for all of them is the release of water molecules.

TH-PM-N4 THE IN VITRO ASSEMBLY OF TOBACCO MOSAIC VIRUS. Robley C. Williams, Virus Laboratory, University of California, Berkeley, California 94720.

A review will be presented of what is currently known about the assembly of tobacco mosaic virus.

TH-PM-N5 CYTOPLASMIC ACTIN AND MYOSIN. Thomas D. Pollard, Anatomy Department, Harvard Medical School, Boston, Massachusetts 02115.

Actin and myosin are components of many non-muscle cells. The actins exist in high concentration and closely resemble muscle actin in primary and filament structure, and in the way they bind myosin. They are relatively thermolabile, however; actin from several types of cells undergoes a temperature-dependent polymerization that results in the gelation of crude extracts. Myosins from vertebrate non-muscle cells, such as platelets and granulocytes, form short thin bipolar filaments in low ionic strength neutral buffers. The myosin heads are loosely attached to the backbone of these filaments, so their arrangement is not evident in electron micrographs of individual filaments. Fortunately, these small filaments can aggregate into paracrystalline tactoids, in which myosin heads on individual filaments exhibit a 15 nm axial periodicity. Using this periodicity and the dimensions of the filaments, one calculates that an average filament consists of 28 myosin molecules, with 2 myosins projecting in each axial repeat. The small size and low concentration in cells of the cytoplasmic myosin filaments may account for their apparent absence in fixed-sectioned cells. These short thin myosin filaments can cross-link actin filaments, forming a structure topologically similar to a muscle sarcomere, so that the structure of the cytoplasmic contractile proteins is consistent with a sliding filament mechanism of force generation. Motile force is presumably generated by the interaction of actin and myosin filaments with the concomitant hydrolysis of ATP, but, in contrast to skeletal muscle myosin, some cytoplasmic myosins require the presence of a third protein to carry out this reaction. This new class of proteins, called cofactors, were originally identified in Acanthamoeba, but have recently been found by Stossel and Hartwig in rabbit macrophages, so they may be a common cellular component.

TH-PM-N6 SEDIMENTATION EQUILIBRIUM STUDIES OF MYOSIN AND C-PROTEIN. R. F. Siemankowski* and P. Dreizen, Department of Medicine and Program in Biophysics, State University of New York Downstate Medical Center, Brooklyn, New York 11203.

High speed sedimentation equilibrium experiments are described on preparations of myosin containing C-protein, and on column-purified myosin (without associated C-protein), under conditions of high ionic strength and neutral pH. The data have been analyzed by the computer program method of Roark and Yphantis. Ultracentrifugal analysis of the preparations containing myosin and C-protein indicates reversible equilibrium dissociation of the complex of myosin and C-protein, at protein concentrations below 1 mg/ml. In addition, small amounts of dimers and higher n-mers are present; analysis of ultracentrifugal data obtained at different loading concentrations and different rotor speeds indicates that this formation of myosin n-mers represents irreversible aggregation, rather than a reversible association, under the solvent conditions employed. Ultracentrifugal studies of column-purified myosin have been performed using interference optical and UV-absorption scanning methods, yielding data to protein concentrations as low as 20 μg/ml. Preliminary analysis of these data indicates that at concentrations below ca. 50 μg/ml, the apparent molecular weight falls below the monomer molecular weight of myosin, consistent with partial dissociation of light chains from the heavy chain core. In addition, there is a substantial increase in the relative amount of irreversible aggregates of myosin, as compared with preparations containing myosin and associated C-protein.

TH-PM-N7 THE MECHANISM OF MICROTUBULE ASSEMBLY IN VITRO. Marc W. Kirschner, Department of Biochemical Sciences, Princeton University, Princeton, New Jersey 08540.

Microtubules appear to assemble and disassemble from small units in vivo. The mechanism of assembly in vitro has been studied by electron microscopy and analytical ultracentrifugation. On depolymerization under a variety of conditions, microtubules release two distinct components sedimenting at 6S and 36S. These appear to be in a concentration dependent equilibrium. Electron microscopic studies reveal that the 36S component is a double ring 480 A in diameter and the 6S component is composed of 70 A globular units. Various experiments indicate that though the 6S and 36S materials are both composed of α- and β-tubulin they are not interconvertible and possess different properties. On polymerizing, all the 36S and 2/3 of the 6S protein is covered into rapidly sedimenting materials which the electron microscope reveals to be microtubules. Quantitative electron microscopic studies indicate that the rings probably convert directly to protofilaments during polymerization using as an intermediate a structure having the form of a helical ribbon. The role of GTP in polymerication has been studied with highly purified protein devoid of a number of enzymic activities contaminating earlier preparations. For such protein, GTP is required for polymerization and a GTPase activity is found to be intrinsic. Studies with the non-hydrolysable analog 5' guanylyl methylene diphosphonate indicate that it can replace GTP in the polymerization process but its effects differ from those of GTP. The results are discussed in terms of a role for GTP binding and hydrolysis in polymerization.

TH-PM-N8 REGULATION OF POLYMERIZATION AND ORGANIZATION OF MICROTUBULES. Richard C. Weisenberg, Department of Biology, Temple University, Philadelphia, Pennsylvania 19122.

Experiments on in vitro assembly of microtubules have suggested possible mechanisms for regulating the assembly and organization of microtubules in the living cell. At approximately physiological concentrations of Mg ions microtubule assembly can be inhibited by micromolar concentrations of Ca, and Ca is a logical candidate to be a microtubule regulator. However, in a system which more closely reflects in vivo assembly of microtubules (formation of aster-like structures in homogenates of surf clam eggs) we have observed that the extent of assembly can apparently be affected by a particulate fraction of the eggs, which is probably the microtubule organizing center. Tubulin subunits, which in the unfertilized egg do not polymerize to any extent, will polymerize if a pellet containing organizing centers is added from dividing cells. Another possible regulatory mechanism involves the formation and activity of types of tubulin aggregates. Ring structures, which can be formed by tubulin, break down during microtubule assembly. However, it is not clear if the presence of rings stimulates or inhibits assembly of microtubules. Evidence will be presented which indicates that the rings exist in competition with microtubules and can therefore inhibit assembly.

TH-PM-N9 VISUALIZATION OF ASSEMBLY AND DISASSEMBLY OF MITOTIC MICROTUBULES. Hidemi Sato*, Prog. in Biophysical Cytology, Department of Biology, Univ. of Pennsylvania, Philadelphia, Pa. 19174.

In addition to their normal assembly into mitotic spindles, spindle microtubule subunits in echinoderm eggs can be crystallized in vivo into two alternate crystalline forms: 1) SM-crystals and 2) VB-crystals. The birefringent SM-crystal, which appear to be a labile liquid crystal, was induced in mature oocytes and gametes by raising temperature or altering the magnesium ion concentration. SM-crystals can readily be transformed from, or to, functional mitotic spindles, but are difficult to stabilize and isolate. The VB-crystal, an irreversibly formed tubulin crystal, is obtained by incubating echinoderm gametes with 10^{-4}M vinblastin sulfate. VB-crystals are produced with a much larger yield per gamete than SM-crystals. The crystal morphology is different, the fine structure is characteristically double helical, and it can be stabilized and isolated in quantity. 10^{-4}M Colcemid mobilizes tubulin and increases the yield of VB-crystal formation. Pure VB-crystals thus isolated from sea urchin gametes was injected into rabbit to induce a tubulin specific antibody. This antibody forms a single band against tubulin purified from Tetrahymena cilia, and from embryonic chick brain in immuno-gel electrophoresis. Fluorescein labelled antibody stained the spindles of rat kangaroo Pt-K2 cells and salamander lung epithelia cells maintained in tissue culture. The fluorescein image provide clear differentiation between microtubular protein organized into spindle fibers and astral rays and amorphous material in the non-birefringent area around the spindle. With fluorescent micrographs we believe we have succeeded in visualizing tubulin in its polymerized form in mitotic microtubules and in an alternate unstructured form. Does this represent the "unpolymerized" form in equilibrium with spindle microtubules? Supported by NIH grant CA-10171 and NSF grant GB-5120.